



**CHALMERS**  
UNIVERSITY OF TECHNOLOGY

## **Extent of Fock-exchange mixing for a hybrid van der Waals density functional?**

Downloaded from: <https://research.chalmers.se>, 2026-06-15 17:09 UTC

Citation for the original published paper (version of record):

Jiao, Y., Schröder, E., Hyldgaard, P. (2018). Extent of Fock-exchange mixing for a hybrid van der Waals density functional?. *Journal of Chemical Physics*, 148(19).  
<http://dx.doi.org/10.1063/1.5012870>

N.B. When citing this work, cite the original published paper.

## Extent of Fock-exchange mixing for a hybrid van der Waals density functional?

Yang Jiao, Elsebeth Schröder, and Per Hyldgaard<sup>a)</sup>

*Department of Microtechnology and Nanoscience (MC2), Chalmers University of Technology, SE-41296 Gothenburg, Sweden*

(Received 8 November 2017; accepted 30 April 2018; published online 21 May 2018)

The vdW-DF-cx0 exchange-correlation hybrid design [K. Berland *et al.*, *J. Chem. Phys.* **146**, 234106 (2017)] has a truly nonlocal correlation component and aims to facilitate concurrent descriptions of both covalent and non-covalent molecular interactions. The vdW-DF-cx0 design mixes a fixed ratio,  $a$ , of the Fock exchange into the consistent-exchange van der Waals density functional, vdW-DF-cx [K. Berland and P. Hyldgaard, *Phys. Rev. B* **89**, 035412 (2014)]. The mixing value  $a$  is sometimes taken as a semi-empirical parameter in hybrid formulations. Here, instead, we assert a plausible optimum average  $a$  value for the vdW-DF-cx0 design from a formal analysis; A new, independent determination of the mixing  $a$  is necessary since the Becke fit [A. D. Becke, *J. Chem. Phys.* **98**, 5648 (1993)], yielding  $a' = 0.2$ , is restricted to semilocal correlation and does not reflect non-covalent interactions. To proceed, we adapt the so-called two-legged hybrid construction [K. Burke *et al.*, *Chem. Phys. Lett.* **265**, 115 (1997)] to a starting point in the vdW-DF-cx functional. For our approach, termed vdW-DF-tlh, we estimate the properties of the adiabatic-connection specification of the exact exchange-correlation functional, by combining calculations of the Fock exchange and of the coupling-constant variation in vdW-DF-cx. We find that such vdW-DF-tlh hybrid constructions yield accurate characterizations of molecular interactions (even if they lack self-consistency). The accuracy motivates trust in the vdW-DF-tlh determination of system-specific values of the Fock-exchange mixing. We find that an average value  $a' = 0.2$  best characterizes the vdW-DF-tlh description of covalent and non-covalent interactions, although there exists some scatter. This finding suggests that the original Becke value,  $a' = 0.2$ , also represents an optimal average Fock-exchange mixing for the new, truly nonlocal-correlation hybrids. To enable self-consistent calculations, we furthermore define and test a zero-parameter hybrid functional vdW-DF-cx0p (having fixed mixing  $a' = 0.2$ ) and document that this truly nonlocal correlation hybrid works for general molecular interactions (at reference and at relaxed geometries). It is encouraging that the vdW-DF-cx0p functional remains useful also for descriptions of some extended systems. *Published by AIP Publishing.* <https://doi.org/10.1063/1.5012870>

### I. INTRODUCTION

An elegant and robust formulation of exchange-correlation (XC) hybrid functionals<sup>1–6</sup> emerges by using the adiabatic-connection formula<sup>7–9</sup> (ACF) to balance exchange and correlation.<sup>10–13</sup> The ACF establishes the XC energy as an integral of the electron-gas response dependence on the assumed strength  $V_\lambda = \lambda V$  of the electron-electron interaction,  $V$ . The  $\lambda = 0$  value is given by Fock exchange  $E_x^{\text{Fo}}$ . The ACF-based hybrid construction is relevant when the hybrid is based on plasmon- and constraint-based XC functionals,<sup>8,9,14–26</sup> where we can use a formal density-scaling analysis<sup>27–29</sup> to reliably extract the nature of the electron-gas response at  $\lambda \rightarrow 1$ . This density and coupling scaling analysis has been completed<sup>11–13,30</sup> for both the semilocal PBE functional<sup>18,31</sup> and for truly nonlocal-correlation functionals of the van der Waals density functional (vdW-DF) method.<sup>20,25,32</sup> The scaling analysis for PBE leads to a rationale for the popular PBE0 hybrid,<sup>2</sup> computing  $E_x^{\text{Fo}}$

from Kohn-Sham (KS) orbitals obtained in a self-consistent solution.

Some of us have recently extended the family of such ACF-based hybrids, launching nonlocal-correlation hybrid formulations, for example, vdW-DF-cx0,<sup>6</sup> based on the consistent-exchange vdW-DF-cx version.<sup>23,33</sup> An exploration of vdW-DF-based hybrids is motivated because the vdW-DF versions still have a generalized gradient approximation (GGA)-type exchange and are thus prone to self-interaction errors.<sup>1,5,11</sup> This limitation affects descriptions of charge-transfer processes in molecular systems.<sup>34,35</sup> Also, the intra-molecular charge transfers affect non-covalent interactions between molecules.<sup>6,36</sup> The vdW-DF-cx0 hybrid is given by

$$E_{xc}^{\text{cx0}} = aE_x^{\text{Fo}} + (1 - a)E_x^{\text{cx}} + E_c^{\text{cx}}, \quad (1)$$

where  $E_{x(c)}$  denotes the exchange (correlation) component of vdW-DF-cx. In launching the original vdW-DF-cx0 version, we picked a fixed Fock-exchange mixing value  $a = 0.25$  in analogy with the construction of PBE0.<sup>2,11</sup> The  $a = 0.25$  choice is different from the  $a' = 0.2$  value that was originally

<sup>a)</sup>hyldgaard@chalmers.se

suggested by Becke for molecular systems<sup>1</sup> and which is used, for example, in the B3LYP hybrid.<sup>3–5</sup>

This paper seeks to answer two questions for the vdW-DF-cx0 design: (1) can we get away with picking a single, all round, value of  $a$  for the study of molecules, and, if so, (2) what would be a good mixing value  $a$ ? The questions are important since the vdW-DF-cx0 design aims to serve as a general purpose materials theory that can deliver concurrent descriptions of both covalent and noncovalent binding in molecules and in bulk. Our analysis is not based on the full ACF-based hybrid construction<sup>10,11,13</sup> (using perturbation-theory studies to establish the  $\lambda \rightarrow 0$  behaviors) for that would be prohibitively costly. Instead we pursue a bootstrap approach, using the so-called two-legged hybrid construction<sup>12,13</sup> to define non-self-consistent (vdW-DF-cx-based) hybrids in a design called vdW-DF-tlh. Such constructions, summarized in Fig. 1 and below, are computationally much cheaper. We simply have to use our previously developed mapping of the coupling-constant scaling for the vdW-DF-cx functional<sup>30</sup> and adapt the original PBE-based analysis.<sup>37</sup> Our vdW-DF-tlh construction can be cast in terms of Eq. (1), however, with the key difference that the Fock-exchange mixing  $a_{\text{sys}}$  is now explicitly asserted for each system and property of interest. From the computed  $a_{\text{sys}}$  values, we can answer our questions around an optimum

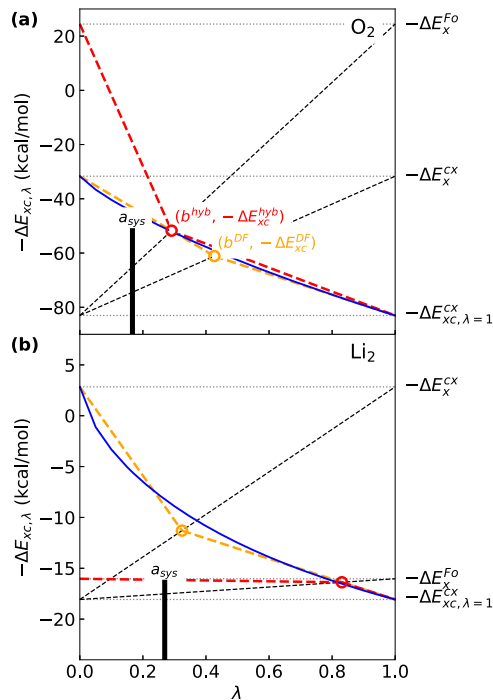


FIG. 1. Constructions of two-legged hybrids, termed vdW-DF-tlh, based on vdW-DF-cx. Here the vdW-DF-tlh approximation is used for analysis of the atomization energies of  $\text{O}_2$  (top panel) and  $\text{Li}_2$  (bottom panel). The panels show the two-legged representations (thick red dashed lines) of the  $\lambda$ -dependence of the exchange-correlation binding contributions.<sup>30</sup> The solid blue curves show the  $\lambda$ -dependence of the vdW-DF-cx exchange-correlation binding contribution. The thin dashed lines are guiding the two-legged-hybrid construction.<sup>12</sup> The orange dashed lines show the two-legged representations of this vdW-DF-cx variation, identifying the weighting  $b^{\text{DF}}$  (orange circles) between contributions evaluated at  $\lambda \rightarrow 0$  and  $\lambda \rightarrow 1$  limits of vdW-DF-cx. The red circles identify the weighting  $b^{\text{hyb}}$  of the  $\lambda \rightarrow 0$  and  $\lambda \rightarrow 1$  limits for a corresponding hybrid-vdW-DF-cx construction. Finally, the pair of vertical thick bars identifies the Fock-exchange mixing value  $a_{\text{sys}}$  that reflects the asserted value of  $b^{\text{hyb}}$ .

average mixing of the Fock exchange in the vdW-DF-cx0 design.

We furthermore consider the question: is there robustness in the vdW-DF-cx0 design? To answer this question, we define a zero-parameter (“0p”) version, termed vdW-DF-cx0p (having Fock mixing  $a' = 0.2$  as motivated by the vdW-DF-tlh analysis). We contrast the performance with that of vdW-DF-cx, the original vdW-DF-cx0 (having Fock mixing  $a = 0.25$ ) version, in self-consistent, fully relaxed calculations. We also compare the performance at reference geometries against that of dispersion-corrected GGA, meta-GGA, and against a traditional (that is, semilocal-correlation) hybrid.<sup>38</sup> Our test cases are molecule systems, subsets of the G2<sup>39</sup> and GMTKN55<sup>38</sup> benchmark sets, bulk semiconductors, and a few transition metals.<sup>40</sup>

The rest of the paper is organized as follows. In Sec. II, we present the theory, summarizing the nature of the ACF-hybrid formulation and of the starting point, the consistent-exchange vdW-DF-cx version.<sup>23,24,33</sup> Section III summarizes computational details and Sec. IV details the two-legged hybrid constructions, defining vdW-DF-tlh. Section V presents our vdW-DF-tlh analysis, discusses a plausible value for the Fock-mixing fraction in the vdW-DF-cx0 hybrid design, and presents a performance comparison. Finally, Sec. VI contains the summary and conclusion.

## II. THEORY

Computing the density-density correlation function  $\chi_\lambda$  at general values of the coupling constant  $\lambda$  for the electron-electron interaction  $\lambda V$  permits a formally exact determination of the XC energy, via the ACF,<sup>7–9</sup>

$$E_{\text{xc}} = - \int_0^\infty \frac{du}{2\pi} \text{Tr}\{\chi_\lambda(iu)V\} - E_{\text{self}}. \quad (2)$$

The last, so-called self-interaction term is just  $E_{\text{self}} = \text{Tr}\{\hat{n}V\}/2$  where  $\hat{n}$  denotes the density operator. For every  $\lambda$ , we can define an XC hole

$$n_{\text{xc},\lambda}(\mathbf{r}, \mathbf{r}') = - \frac{1}{n(\mathbf{r})} \int_0^\infty \frac{du}{2\pi} \chi_\lambda(\mathbf{r}, \mathbf{r}'; iu) - \delta(\mathbf{r} - \mathbf{r}') \quad (3)$$

and an XC energy contribution

$$E_{\text{xc},\lambda} \equiv \frac{1}{2} \int_{\mathbf{r}} \int_{\mathbf{r}'} \frac{n(\mathbf{r}) n_{\text{xc},\lambda}(\mathbf{r}, \mathbf{r}')}{|\mathbf{r} - \mathbf{r}'|}. \quad (4)$$

The exact XC energy then results from a coupling constant integral

$$E_{\text{xc}} = \int_0^1 d\lambda E_{\text{xc},\lambda}. \quad (5)$$

### A. Consistent-exchange vdW-DF

The vdW-DF method<sup>6,20,21,23–25,32,41,42</sup> is an attractive framework for approximating the XC energy in density functional theory (DFT). The method starts by considering the XC holes of a generalized gradient approximation (GGA) functional.<sup>20,21</sup> It then adds a truly nonlocal correlation term  $E_c^{\text{nl}}$  that systematically counts the total energy gain by the electrodynamic coupling between such semilocal XC holes.<sup>24,43–46</sup>

The family of vdW-DF versions and variants<sup>20,23,42,47–51</sup> permits computationally efficient<sup>52–54</sup> DFT studies of sparse materials,<sup>55</sup> systems which have important regions with a low electron density. These truly nonlocal functionals have by now found very broad applications, as summarized in Refs. 32, 55, and 56. The same is true for the related VV09 and VV10 functionals<sup>22,57,58</sup> that use a different screening model for the account of nonlocal correlation effects.

In the vdW-DF method, we split the XC energy into a semilocal GGA-type functional  $E_{xc}^0$  and a truly nonlocal-correlation term  $E_c^{nl}$ . In general, there is also a crossover term  $\delta E_x^0$  related to the exchange description, as discussed elsewhere,<sup>23,24,32,33</sup>

$$E_{xc}^{vdW-DF} = E_{xc}^0 + E_c^{nl} + \delta E_x^0. \quad (6)$$

The vdW-DF method can be interpreted as a computationally efficient evaluation of the coupling-induced frequency shifts in the Ashcroft picture of vdW forces.<sup>24,43–46</sup> The long-range vdW forces are described as arising from an electron-dynamical coupling between GGA-type XC holes and in the presence of the screening produced by the surrounding atoms.<sup>24</sup>

The recent consistent-exchange vdW-DF-cx version<sup>23</sup> is crafted so that it preserves current in its account of the electron-gas response.<sup>33</sup> In practical terms, the consistent-exchange vdW-DF-cx formulation seeks to eliminate the adverse effects of the crossover term  $\delta E_x^0$  in Eq. (6), making it effectively an approximate mean-value evaluation<sup>23,24</sup> of the ACF.<sup>7–9</sup> This is possible as long as the interaction is dominated by contributions with small values of the density gradient.<sup>23,24,30,59</sup> The vdW-DF-cx performs on par with or better than the popular GGAs<sup>18,19</sup> for many bulk, surface, interface, and molecular properties.<sup>6,60–76</sup> It reliably accounts for van der Waals (vdW) forces in cases where interactions compete,<sup>33,77</sup> for example, in the descriptions of weak chemisorption, oxide ferroelectrics, and metal-organic frameworks.<sup>25,33,78,79</sup>

## B. Coupling constant scaling and hybrids

Use of hybrid XC functionals in DFT is in general motivated by the observation that the exchange dominates in several molecular properties. A semilocal exchange form often leads to too much confinement<sup>1,5</sup> of the so-called XC hole<sup>8,9</sup> that reflects this electron-gas response. The coupling-constant analysis of physically motivated functionals<sup>10–13,27,28,30</sup> permits us to pursue an ACF-based hybrid construction.

The key observations are these. At physical conditions, corresponding to  $\lambda = 1$ , the plasmons dominate the  $\chi_{\lambda=1}$  behavior for homogeneous systems.<sup>80</sup> The same is expected to hold in the weakly perturbed electron gas.<sup>14</sup> Like the early formulations of the local-density approximation (LDA),<sup>8,9,81</sup> the consistent-exchange vdW-DF-cx explicitly emphasizes a plasmon foundation in its characterization of response  $\chi_{\lambda}$  in the screened electron gas.<sup>25,33,60</sup> This is done by crafting both exchange and correlation terms from a single-pole response model.<sup>24</sup> A benefit is that we can expect  $E_{xc,\lambda}^{vdW-DF}$  to provide an accurate account in the  $\lambda \rightarrow 1$  limit. However, in the

$\lambda \rightarrow 0$  limit, the response  $\chi_0$  must be different, given exclusively by single-particle excitation and exchange effects. In summary, we are motivated to extend the vdW-DF-cx design with a hybrid formulation, such as the recently formulated unscreened hybrid vdW-DF-cx0.<sup>6</sup>

A more complete discussion is available by starting from the vdW-DF-cx coupling-constant scaling.<sup>30</sup> Here we just summarize the principle and the results that are relevant for the discussion of a hybrid vdW-DF-cx formulation. The essential part is this result: using the simple density scaling

$$n(\mathbf{r}) \rightarrow n_{1/\lambda}(\mathbf{r}) \equiv n(\mathbf{r}/\lambda)/\lambda^3, \quad (7)$$

we can trace out the full coupling-constant variation using

$$E_{xc,\lambda}[n] = \frac{d}{d\lambda} \left\{ \lambda^2 E_{xc}[n_{1/\lambda}] \right\}. \quad (8)$$

The solid curves in Fig. 1 show the corresponding coupling constant scaling as it emerges for the XC energy contribution to the binding in the O<sub>2</sub> and Li<sub>2</sub> dimers. The relevant quantity in typical DF theory calculations is energy differences, for example, the difference between the molecule and atom total energies,

$$\Delta E^{DF} = \sum_i E_{atom,i}^{DF} - E_{mol}^{DF}. \quad (9)$$

To discuss a hybrid formulation, we focus on the corresponding changes in the XC contributions  $\Delta E_{xc}[n]$  as well as on the differences that arise upon mapping the coupling constant scaling,  $\Delta E_{xc,\lambda}^{DF}$ , and taking the  $\lambda \rightarrow 1$  limit. For the hybrid vdW-DF constructions, we also need to compute binding-energy contributions,  $\Delta E_{xc}^{DF}$ , arising from the DF exchange (correlation) components.

The full ACF-based hybrid construction<sup>10</sup> provides a formal argument that the Fock mixing in a hybrid construction (aiming to compute, for example, atomization energies) should be chosen in the form<sup>11–13</sup>  $a = 1/m$ , for  $m = 3, 4, 5, \dots$ . The integer  $m$  reflects the nature<sup>11</sup> of the perturbation-theory calculation that enters in the full ACF-based hybrid construction.<sup>10</sup> The value of  $m$  and thus  $a$  will, in principle, depend on both the system and the property that one wishes to investigate (as well as on the choice of the underlying functional). On the other hand, the hybrid PBE0 and the hybrid vdW-DF-cx0, Eq. (1), are only truly useful for making material-specific predictions (of structure and binding) when they are deliberately kept free of parameters. Typically, hybrid GGAs are used following the recommendation<sup>82</sup> to stick with a fixed value of  $a$  (one of the typical choices  $a = 0.25$  or  $a = 0.2$ ) since such choices are consistent with the formal nature of a full ACF-based hybrid construction.<sup>11</sup>

Here, we argue that the same approach should be used for vdW-DF-based hybrid constructions, including vdW-DF-cx0 that is based on vdW-DF-cx.<sup>6</sup> Our discussion is based on crafting system-specific approximations to the full ACF-based hybrid construction,<sup>10,11,13</sup> adapting the ideas of the two-legged hybrid constructions for PBE.<sup>12</sup> Our approximation scheme, termed vdW-DF-tlh, permits us to discuss if a good (average)  $a$  value can be found for using the vdW-DF-cx0 design<sup>6</sup> on problems defined by general (covalent and non-covalent) interactions.

### III. COMPUTATIONAL DETAILS

All of our calculations are based on the plane wave QUANTUM ESPRESSO package<sup>83,84</sup> which has the consistent exchange vdW-DF-cx version,<sup>23</sup> as well as the rigorous spin extension of the vdW-DF method.<sup>25</sup> All molecule studies use an 80 Ry wavefunction-energy cutoff. Core electrons are generally represented by Troullier-Martins type<sup>85</sup> norm-conserving pseudo potentials from the ABINIT package<sup>86</sup> in our studies of molecular properties. However, we used the QUANTUM ESPRESSO projector augmented-wave (PAW) setup<sup>87</sup> to also complete a set of PBE-XDM<sup>88,89</sup> studies that we present in a performance comparison.

For the vdW-DF-tlh construction, we rely on a numerical analysis of the coupling-constant scaling of density functional components, evaluating Eq. (8). Here we use a post-processing code, termed `PPACF`, that we have described separately.<sup>30</sup> As summarized below, we need to only compute the differences in the  $E_{xc,\lambda=1}$  values (as obtained for given densities).

An  $8 \times 8 \times 8k$ -point sampling and optimized norm-conserving Vanderbilt (ONCV) pseudopotentials<sup>90</sup> are used for our vdW-DF-cx and vdW-DF-cx0(p) characterizations of bulk semiconductors and of a few transition metals.

We systematically rely on the adaptively compressed exchange (ACE) operator<sup>91</sup> for calculations of the Fock-exchange term  $\Delta E_x^{F_0}$ . This is now a standard part of QUANTUM ESPRESSO<sup>84</sup> (although requiring a pre-compilation flag). Use of ACE speeds up hybrid calculations for molecules and it dramatically accelerates hybrid studies of extended systems.<sup>91</sup> The ACE acceleration makes it possible to complete a self-consistent hybrid DFT calculation of a transition-metal element on the scale of hours (on a single, standard node of a high-performance computer).

### IV. HYBRID CONSTRUCTION: vdW-DF-tlh

The hybrids rely on calculations of the Fock-exchange energy

$$E_x^{F_0} = -\frac{1}{2} \int_{\mathbf{r}} \int_{\mathbf{r}'} \frac{\tilde{n}_1(\mathbf{r}, \mathbf{r}') \tilde{n}_1(\mathbf{r}', \mathbf{r})}{|\mathbf{r} - \mathbf{r}'|}, \quad (10)$$

where  $n_1(\mathbf{r}, \mathbf{r}') = \sum_i \phi_i^*(\mathbf{r}) \phi_i(\mathbf{r}')$  and where  $\phi_i$  denotes the set of solution wavefunctions. Fock-energy differences,  $\Delta E_x^{F_0}$ , defined in analogy with Eq. (9), are mixed with the exchange description of the underlying density function (in our case vdW-DF-cx) to correct the description of, for example, band gaps and self-interaction effects. For standard hybrid calculations, the wavefunctions  $\phi_i$  are taken as the KS solutions. For discussion of atomization energies, however, we found that it was necessary to assert  $\Delta E_x^{F_0}$  from self-consistent Hartree-Fock solutions.

#### A. Two-legged hybrid approximation

We first recall that any regular density functional “DF” should itself be seen as providing a crossover between approximations for the single-particle and for the many-particle descriptions at  $\lambda = 0$  and  $\lambda = 1$ , respectively.<sup>12</sup> For the pure functional, we simply inquire when the  $\lambda$  scaling of vdW-DF-cx, or of any functional “DF,” intersects the opposite diagonal<sup>12</sup>  $[0, E_{xc,\lambda=1}^{DF}] - [1, E_x^{DF}]$  at  $[b^{DF}, E_{xc}^{DF}]$ .

The intersection point,

$$b^{DF}[n] = \frac{E_{xc}^{DF}[n] - E_{xc,\lambda=1}^{DF}[n]}{E_x^{DF}[n] - E_{xc,\lambda=1}^{DF}[n]}, \quad (11)$$

determines the weighting of  $\lambda \rightarrow 0$  and  $\lambda \rightarrow 1$  components

$$E_{xc}^{DF}[n] = b^{DF}[n] E_x^{DF}[n] + (1 - b^{DF}[n]) E_{xc,\lambda=1}^{DF}[n]. \quad (12)$$

Note that  $b^{DF}[n]$  is itself a functional of the density—but that is just a part of the overall “DF” description. For a description of “DF” energy differences,

$$\Delta E_{xc}^{DF} = b_{\text{sys}}^{DF} \Delta E_x^{DF} + (1 - b_{\text{sys}}^{DF}) \Delta E_{xc,\lambda=1}^{DF}, \quad (13)$$

there is, consequently, an explicit system dependence on the weighting,  $b_{\text{sys}}^{DF}$ , of  $\lambda \rightarrow 0$  and  $\lambda \rightarrow 1$  contributions, as indicated by the subscript “sys.”

The hybrid vdW-DF-cx constructions should be seen as a natural generalization of the regular-functional mixing behavior Eq. (13); the generalization is motivated by the fact that the Fock-exchange differences  $\Delta E_x^{F_0}$ , Eq. (10), are generally more accurate than the DF exchange description. The two-legged non-empirical hybrid constructions<sup>11,12</sup> use  $\Delta E_x^{F_0}$  to anchor the  $\lambda \rightarrow 0$  limit, expressing a corrected weighting

$$\Delta E_{xc}^{\text{hyb}} = b_{\text{sys}}^{\text{hyb}} \Delta E_x^{F_0} + (1 - b_{\text{sys}}^{\text{hyb}}) \Delta E_{xc,\lambda=1}^{DF}. \quad (14)$$

By establishing the new weighting factors  $b_{\text{sys}}^{\text{hyb}} \neq b_{\text{sys}}^{DF}$ , below, we also determine rational choices for the mixing of a Fock exchange term as expressed in a more common hybrid construction form

$$\Delta E_{xc}^{\text{hyb}} = a_{\text{sys}} \Delta E_x^{F_0} + (1 - a_{\text{sys}}) \Delta E_x^{DF} + E_c^{DF}. \quad (15)$$

The formal relation to Eq. (14) is given by

$$a_{\text{sys}} = \frac{\Delta E_{xc}^{\text{hyb}} - \Delta E_{xc}^{DF}}{\Delta E_x^{F_0} - \Delta E_x^{DF}}. \quad (16)$$

For the two legged constructions,<sup>12</sup> we define and approximate two gradients,

$$g_{\text{sys}}^L = \left. \frac{d\Delta E_{xc,\lambda}}{d\lambda} \right|_{\lambda=0} \approx -\frac{\Delta E_x^{DF} - \Delta E_{xc}^{DF}}{b_{\text{sys}}^{DF}}, \quad (17)$$

$$g_{\text{sys}}^R = \left. \frac{d\Delta E_{xc,\lambda}}{d\lambda} \right|_{\lambda=1} \approx -\frac{\Delta E_{xc}^{DF} - \Delta E_{xc,\lambda=1}^{DF}}{1 - b_{\text{sys}}^{DF}}. \quad (18)$$

The first gradient should ideally be computed in perturbation theory, leading to the non-empirical hybrid construction discussed in Ref. 11; An exploration of this approach is beyond the present scope. Both gradients are instead approximated, as indicated, by a linear form given by  $b_{\text{sys}}^{DF}$ , namely, the position of the kink in a two-legged construction for vdW-DF-cx itself.

Besides the vdW-DF-cx energy differences, we also compute the Fock exchange energy difference to provide a vdW-DF-cx- and system-specific determination of  $g_{\text{sys}}^L$  (and  $g_{\text{sys}}^R$  when relevant). Adapting the logic of Ref. 12, the value of  $g_{\text{sys}}^L$  specifies a motivated approximation for balancing  $\lambda \rightarrow 0$  and  $\lambda \rightarrow 1$  contributions in cases where  $\Delta E_x^{F_0} < \Delta E_x^{DF}$ . The value of  $g_{\text{sys}}^R$  is only relevant for cases where  $\Delta E_x^{F_0} > \Delta E_x^{DF}$  and its use requires an additional discussion, given below.

The top panel of Fig. 1 illustrates the vdW-DF-tlh construction for a typical molecular-binding case, binding in the O<sub>2</sub> molecule. The orange circle identifies the crossing point between the vdW-DF-cx coupling-constant scaling (blue curve) and the diagonal (lower black dotted line) from ( $\lambda = 0, -\Delta E_{xc,\lambda=1}$ ) to ( $\lambda = 1, -\Delta E_x^{\text{DF}}$ ). The crossing point ( $\lambda = b_{\text{sys}}^{\text{DF}}, -\Delta E_{xc}^{\text{DF}}$ ) is system and property specific, with the value of  $b_{\text{sys}}^{\text{DF}}$  given by the generalization of Eq. (11) to energy differences. The dashed orange curve shows a two-legged approximation for the actual DF coupling constant variation; this curve has a kink at the orange circle.

Figure 1 summarizes our vdW-DF-tlh constructions. The figure shows that there are differences between the Fock and DF exchange binding contributions,  $\Delta E_x^{\text{Fo}}$  and  $\Delta E_x^{\text{DF}}$ . We seek revised coupling-constant curves that better approximate the coupling-constant variation in the ACF determination of the exact XC functional. The  $\Delta E_x^{\text{Fo}} - \Delta E_x^{\text{DF}}$  difference is used to define two-legged constructions,<sup>12</sup> for example, the red dashed curves in Fig. 1, anchored by  $-\Delta E_x^{\text{Fo}}$  in the  $\lambda \rightarrow 0$  limit and the trusted  $-\Delta E_{xc,\lambda=1}$  value at the other end. In essence, we first use Eq. (14) to complete the vdW-DF-tlh calculation of the energy difference and we then use Eq. (15) to extract the mixing  $a_{\text{sys}}$  that is equivalent to this vdW-DF-tlh description.

Our two-legged hybrid constructions seek to follow the DF coupling-constant scaling as far as possible as we move to lower coupling constant values.<sup>12</sup> This leads to placing the kink (red circle) in the revised two-legged curve (dashed red curve) both on the vdW-DF-cx coupling constant curve and on the second indicated diagonal (upper black dotted line). The intersection or kink (red circle) identifies the plausible value of a revised weighting<sup>12</sup>

$$b_{\text{sys}}^{\text{hyb,L}} = \frac{\Delta E_x^{\text{DF}} - \Delta E_{xc,\lambda=1}^{\text{DF}}}{\Delta E_x^{\text{Fo}} - \Delta E_{xc,\lambda=1}^{\text{DF}} - g_{\text{sys}}^{\text{L}}} \quad (19)$$

of  $\lambda \rightarrow 0$  and  $\lambda \rightarrow 1$  limits. In this case, the revised two-legged approximation suggests that the plausible coupling-constant curve would also be downward concave. The  $\lambda$  value  $b_{\text{sys}}^{\text{hyb,L}}$  will be located to the left of  $b_{\text{sys}}^{\text{DF}}$ , as identified by the superscript. The  $b_{\text{sys}}^{\text{hyb,L}}$  is finally converted into a system (and property) specific value of a plausible Fock-exchange mixing value  $a_{\text{sys}}$ , given by Eq. (16), and as identified by the thick vertical bar.

The lower panel shows how we have adapted the two-legged constructions for descriptions of the atomization energies for Li<sub>2</sub>, LiH, and OH and for other cases where  $E_x^{\text{Fo}} > E_x^{\text{DF}}$ . Aiming again to align the coupling constant scaling behavior in the large- $\lambda$  limit, we then place the kink (red circle) of the revised two-legged approximation (red dashed line) at  $(b_{\text{sys}}^{\text{hyb,R}}, \Delta E_{\text{Fo}}^{\text{DF}})$ , where

$$b_{\text{sys}}^{\text{hyb,R}} = \frac{-g_{\text{sys}}^{\text{R}}}{\Delta E_x^{\text{Fo}} - \Delta E_{\text{Fo},\lambda=1}^{\text{DF}} - g_{\text{sys}}^{\text{R}}}. \quad (20)$$

That is, in such adjusted two-legged constructions,  $b_{\text{sys}}^{\text{hyb,R}}$  is the  $\lambda$  value that formally specifies the weighting of  $\lambda \rightarrow 0$  and  $\lambda \rightarrow 1$  limits. As indicated by the superscript ‘‘R,’’ we then have

$b_{\text{sys}}^{\text{hyb,R}} > b_{\text{sys}}^{\text{DF}}$ , leading to larger values of the corresponding Fock-exchange mixing value  $a_{\text{sys}}$ .

Table I summarizes the vdW-DF-tlh constructions, showing the  $a_{\text{sys}}$  and atomization-energy results. The table focuses on the systems that were originally analyzed for two-legged hybrid constructions based on PBE.<sup>12</sup> We find that there is a spread in the predicted values of  $a_{\text{sys}}$ . We also find that the binding energies  $\Delta E^{\text{tlh}}$  that are predicted with vdW-DF-tlh improve the description relative to that provided by the vdW-DF-cx starting point. However, it is important to point out that the vdW-DF-tlh constructions are introduced for analysis purposes only.

## B. Limitations of vdW-DF-tlh usage

There are four fundamental and practical problems with using vdW-DF-tlh. First, it cannot be cast in a self-consistent formulation and thus cannot be used for general material characterizations nor will it always be accurate.<sup>12</sup> Second, the design logic breaks down completely when  $-\Delta E_x^{\text{Fo}}$  is lower than  $-\Delta E_{xc,\lambda}^{\text{DF}}$ . Third, it is not clear that the two-legged construction holds for cases where it implies using a small value of the Fock mixing ratio,  $a_{\text{sys}} < 0.15$ , in Eq. (15), for reasons discussed in Refs. 11–13. Fourth, in cases where  $E_x^{\text{Fo}} < E_x^{\text{DF}}$  (for example, as in the bottom panel of Fig. 1), it is not easy to motivate the particular vdW-DF-tlh description as a plausible approximation to the exact ACF XC-functional specification<sup>8,9</sup> or even to the full ACF-based hybrid construction.<sup>10</sup>

The last point deserves an additional discussion as it impacts our analysis. The coupling constant variation in  $E_{xc,\lambda}$  should be downward concave in the exact ACF evaluation.<sup>27–29</sup> This downward-concave behavior is correctly reflected in the coupling-constant variations that represent the vdW-DF-cx functional behavior. With a full ACF-based hybrid construction,<sup>10</sup> we would also expect a downward concave coupling constant variation, having a form similar to that shown by the red dashed line in the top panel of Fig. 1.

However, the approximate, non-self-consistent vdW-DF-tlh construction sometimes produces an upward concave coupling-constant variation, the bottom panel of Fig. 1. Such variations, for the specific vdW-DF-tlh constructions, are not motivated by formal theory,<sup>28,29</sup> even if these vdW-DF-tlh constructions are themselves fairly accurate in characterizations of atomization energies, molecular-reaction energies, and ionization potential energies (Tables S.I, S.III, and S.IV of the [supplementary material](#), respectively). Interestingly, the issue does not appear in the vdW-DF-tlh description of our set of non-covalent inter-molecular bonding, Table S.V of the [supplementary material](#).

We interpret this practical problem for vdW-DF-tlh usage for characterization of standard molecular properties (atomization, reaction, and ionization energies) as a warning of insufficient accuracy in the two-legged constructions. We note that vdW-DF-tlh is not self-consistent so we need to have a plausible guess for the character of the wavefunctions when computing the Fock-exchange term. In hybrid-DFT calculations, we generally use KS wavefunctions (here obtained in self-consistent vdW-DF-cx calculations), but these are not directly relevant for a characterization of the Fock-exchange

TABLE I. Exchange-correlation contribution to atomization energies of molecules, in kcal/mol (1 eV = 23.06 kcal/mol). “cx” is short for vdW-DF-cx. All results are obtained for coordinates fixed in MP2(full)/6-31G(d) optimized geometries,<sup>39</sup> and calculations are thus lower bounds on the atomization energies. The test group is that used in Ref. 12 to discuss the original PBE-based two-legged hybrid construction. The table also summarizes the performance in terms of mean deviation (MD), mean absolute deviation (MAD), and mean absolute relative deviation (MARD) values.

Molecule	$\Delta E^{\text{ref}}$	$\Delta E^{\text{cx}}$	$\Delta E_x^{\text{HF}}$	$\Delta E_x^{\text{cx}}$	$\Delta E_{\text{xc}}$	$\Delta E_{\text{xc}, \lambda=1}^{\text{cx}}$	$a_{\text{sys}}$	$\Delta E^{\text{tlh}}$
LiH	58	58	31	28	51	64	0.13	58
CH <sub>4</sub>	420	429	168	222	307	362	0.21	418
NH <sub>3</sub>	298	303	82	127	202	252	0.21	293
OH	106	105	31	28	55	73	0.17	106
H <sub>2</sub> O	233	237	67	110	160	193	0.20	228
HF	141	145	39	74	98	115	0.18	139
Li <sub>2</sub>	24	19	16	-3	11	18	0.27	24
LiF	138	140	111	124	148	165	0.21	137
C <sub>2</sub> H <sub>2</sub>	406	417	112	237	310	361	0.17	395
C <sub>2</sub> H <sub>4</sub>	563	579	212	326	436	510	0.19	557
HCN	313	320	11	125	188	232	0.17	301
CO	259	265	5	101	137	164	0.15	251
N <sub>2</sub>	228	228	-96	6	59	97	0.17	211
NO	153	161	-41	30	73	105	0.17	148
Cl <sub>2</sub>	58	70	-18	60	77	89	0.11	61
O <sub>2</sub>	120	138	-24	32	61	83	0.17	128
H <sub>2</sub>	110	112	23	30	57	73	0.22	110
F <sub>2</sub>	38	52	-95	10	27	41	0.10	42
P <sub>2</sub>	117	120	-68	-13	30	60	0.18	110
Average $a_{\text{sys}}$							0.18	
MD (kcal/mol)		5.95						-3.45
MAD (kcal/mol)		6.68						5.02
MARD (%)		6.47						2.89

energies of atom and molecules. They will not always produce  $\Delta E_x^{\text{F}0}$  estimates that are accurate.

Table S.II of the [supplementary material](#) shows a vdW-DF-tlh characterization of atomization energies, when instead we use self-consistent Hartree-Fock calculations to determine the Fock-exchange energy. The table shows that this adjustment in the two-legged hybrid construction ensures that a downward concave variation underpins the vdW-DF-tlh analysis for atomization energies for all but four cases. One of these exceptions is the case of the Li dimer, the specific example that we analyze in the bottom panel of Fig. 1. Computing  $\Delta E_x^{\text{F}0}$  from Hartree-Fock solution wavefunctions is, on the other hand, not motivated for the study of the reaction or of general ionization energies.

We base our analysis of the vdW-DF-cx0 design, below, on vdW-DF-tlh constructions in which  $\Delta E_x^{\text{F}0}$  is computed from vdW-DF-cx wavefunctions for all but the atomization energies (where we use HF). This means including cases with an upward concave scaling behavior, for example, in the case of reaction and ionization energies (Tables S.II–S.IV of the [supplementary material](#)). The impact on our analysis and for the predictions for an average mixing value  $a_{\text{sys}}$ , however, is limited. For molecular atomization, reaction, and ionization energies (Tables S.II–S.IV of the [supplementary material](#)), the set of vdW-DF-tlh constructions suggest an average Fock mixing value  $a = \langle a_{\text{sys}} \rangle = 0.186 \approx 0.2$  for the vdW-DF-cx0 design.<sup>6</sup> If instead we had restricted the analysis set to

cases with a resulting downward-concave coupling-constant variation,<sup>12,28,29</sup> the average would be  $\langle a_{\text{sys}} \rangle = 0.178$ .

## V. RESULTS AND DISCUSSIONS

The usefulness of our two-legged hybrid vdW-DF-cx constructions is that they provide analysis of the nature of and the extent of exchange mixing  $a = 1/m$  in the vdW-DF-cx design.<sup>6</sup> We note that the formal ACF-based hybrid construction<sup>10,11,13</sup> motivates that we should pick  $m = 4$ ,  $m = 5$ , or perhaps  $m = 6$ .<sup>94</sup>

A necessary condition for using our vdW-DF-tlh constructions for an analysis of the vdW-DF-cx0 design is that the vdW-DF-tlh characterizations can be seen as accurate. In the following, we therefore list a summary of the vdW-DF-tlh constructions and of the asserted average mixing values  $\langle a_{\text{sys}} \rangle$ , in concert with statistical analysis of performance for molecular interactions, as compared against quantum-chemistry reference calculations.<sup>38,39,95</sup>

Overall, we present and summarize vdW-DF-tlh constructions for atomization energies (the G2-1 set, Table S.II of the [supplementary material](#)), for reaction energies (subset of G2RC, Table S.III of the [supplementary material](#)), for ionization energies (subset of G2IIP, Table S.IV of the [supplementary material](#)), for inter-molecular non-covalent interactions (S22, Table S.V of the [supplementary material](#)), for intra-molecular non-covalent interactions (IDISP, Table S.VI of the

supplementary material), for binding energies of aluminum dimers (Al2X6, S.VII of the supplementary material), and for a set of Diels-Alder reaction energies (DARC, Table S.VIII of the supplementary material), using reference geometries and reference binding energies in the G2<sup>39</sup> and the GMTKN55<sup>38</sup> benchmark sets. For each of the benchmark (and construction) subsets, we report the vdW-DF-tlh specification of the averaged Fock-exchange mixing parameter  $\langle a_{\text{sys}} \rangle$ , the mean deviation (MD), mean absolute deviation (MAD), and mean absolute relative deviation (MARD) values that characterize the vdW-DF-tlh constructions.

Figure 2 shows representative examples of the IDISP, Al2X6, and DARC benchmark sets. We include these benchmark sets because they are expected to reflect effects of the electron affinity and delocalization errors on both non-covalent and covalent molecular binding and thus challenge hybrid formulations.<sup>95</sup> The intra-molecular non-covalent IDISP set has a low average absolute relative energy of about 14 kcal/mol<sup>38</sup> and represents cases where the weaker vdW interaction competes with other binding mechanisms.<sup>33,60</sup> The DARC sets are defined from systems also involving double and triple bonds. Here one might expect a better performance from a meta-GGA (like SCAN<sup>96</sup> or dispersion-corrected versions thereof<sup>26,38</sup>) than from a standard hybrid.<sup>95</sup> They are important tests on our analysis of and search for a plausible average value of the Fock-exchange mixing parameter  $\langle a_{\text{sys}} \rangle$  in the vdW-DF-cx0 design.<sup>6</sup> They allow us to test if the average  $\langle a_{\text{sys}} \rangle \approx 0.2$  obtained by the vdW-DF-tlh analysis of atomization, reaction, and ionization cases (discussed in Sec. IV A) also holds in more general molecular interaction cases.

### A. Summary of vdW-DF-tlh constructions and performance

Table II reports an overview of the performance of vdW-DF-tlh, compared with that of PBE0 and of vdW-DF-cx itself

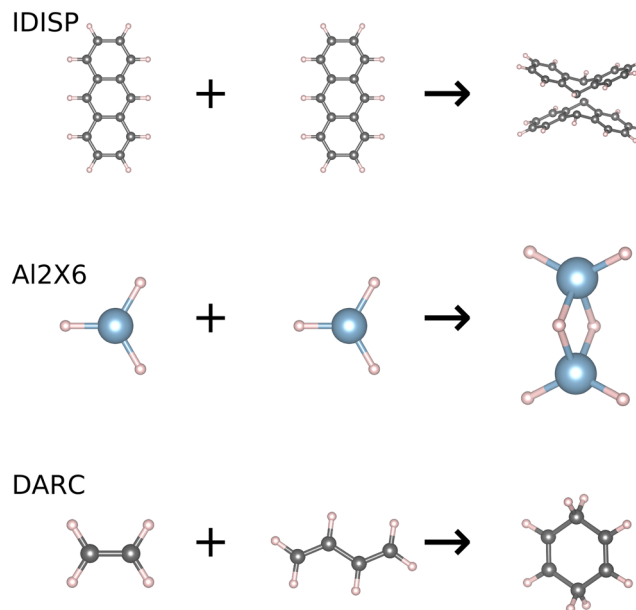


FIG. 2. Tests of the role of charge relocation in general molecular interaction: representative examples from the benchmark sets<sup>38</sup> of intra-molecular non-covalent binding (IDISP, top row) of aluminum dimerization (Al2X6, middle row) and of Diels-Alder reaction energies (DARC, bottom row).<sup>38</sup>

and as obtained for a range of benchmarks for covalent molecular binding. The table also lists the average of the  $a_{\text{sys}}$  values that results in the two-legged constructions. The distribution of such  $a_{\text{sys}}$  values centers on  $\langle a_{\text{sys}} \rangle = 0.2$ . However, there is also some scatter in the vdW-DF-tlh specification of  $a_{\text{sys}}$  values, as seen in Tables S.II and S.III of the supplementary material.

Table II shows that, overall, the performance of vdW-DF-tlh is good for covalent molecular binding properties, as compared with PBE0, with vdW-DF-cx, and with the original vdW-DF-cx0 version.<sup>6</sup> To provide a fair comparison,

TABLE II. Summary of two-legged hybrid construction and comparison of performance for the 55 molecule atomization energies of the G2-1 data set,<sup>39</sup> for 17 molecular reaction energies in the G2RC data set,<sup>38</sup> and for 26 ionization potentials in the G21IP data set.<sup>38</sup> All energies are in kcal/mol (1 eV = 23.06 kcal/mol). “cx” is short for vdW-DF-cx. The results are evaluated at coordinates fixed in MP2(full)/6-31G(d) optimized geometries for G2-139 and at experimental geometries for G2RC and for G21IP.<sup>38</sup> The Fock exchange terms are calculated using the orbitals of Hartree-Fock (vdW-DF-cx) calculations for G2-1 (for G2RC and for G21IP). The average mixing ratios,  $a_{\text{sys}}$ , are 0.18, 0.21, and 0.18, respectively.

Molecule	$\Delta E^{\text{PBE0}}$	$\Delta E^{\text{cx}}$	$\Delta E^{\text{tlh}}$	$\Delta E^{\text{cx0}}$	$\Delta E^{\text{cx0p}}$
G2-1 atomization	$a = 0.25$	$a = 0$	$\langle a_{\text{sys}} \rangle = 0.18$	$a = 0.25$	$a' = 0.20$
MD (kcal/mol)	-4.37	8.28	-1.46	-2.85	-0.61
MAD (kcal/mol)	5.50	8.94	4.29	5.58	4.18
MARD (%)	4.42	6.47	2.98	4.17	3.24
G2RC subset (17 reactions)	$a = 0.25$	$a = 0$	$\langle a_{\text{sys}} \rangle = 0.21$	$a = 0.25$	$a' = 0.20$
MD (kcal/mol)	-3.80	-0.10	-1.80	-2.34	-1.89
MAD (kcal/mol)	5.68	5.78	4.90	4.43	4.54
MARD (%)	38.03	57.08	38.55	35.10	38.46
G21IP subset (26 molecules)	$a = 0.25$	$a = 0$	$\langle a_{\text{sys}} \rangle = 0.18$	$a = 0.25$	$a' = 0.20$
MD (kcal/mol)	-1.22	-2.67	-3.43	-0.02	-0.32
MAD (kcal/mol)	5.27	4.25	5.57	4.19	4.22
MARD (%)	2.16	1.66	2.28	1.75	1.76

the table lists PBE0, vdW-DF-cx, and vdW-DF-cx0 results for energies at the reference geometries that were also used in the vdW-DF-tlh characterizations; we shall return to a discussion of relaxation effects below. The MD, the MAD, and the MARD decrease for the set of G2-1 atomization energies. The vdW-DF-tlh remains comparable to the performance of PBE0 and vdW-DF-cx0 for the subset of reaction energies. The vdW-DF-tlh performance for ionization energies seems to slightly worsen, however, likely because the absence of a self-consistent determination affects the orbital description.

Table III reports a summary of the two-legged construction and a comparison of the vdW-DF-tlh performance for the S22 benchmark set,<sup>92,99</sup> focusing on inter-molecular

binding energies. The table is divided into cases with hydrogen, dispersion, and mixing bonding cases but also summarizes the overall performance as compared to vdW-DF-cx and to vdW-DF-cx0, Ref. 6. Again, there is some scatter in the predicted plausible  $a_{\text{sys}}$  values but the average is centered on 0.2. The performance of vdW-DF-tlh is better than that of vdW-DF-cx0 in which the good account of hydrogen bonding is preserved, while vdW-DF-tlh avoids some of the errors that vdW-DF-cx0 makes for purely vdW bonded cases.<sup>6</sup>

Table IV shows a summary of the vdW-DF-tlh construction as well as a performance comparison for the IDISP, A12X, and DARC benchmark sets.<sup>95</sup> There is for these additional vdW-DF-tlh construction cases only a small scatter of the

TABLE III. Binding energies of the S22 data set. The geometries are optimized at either the CCSD(T) or MP2 level as taken from Ref. 92. The reference interaction energies are taken from Ref. 93 as suggested by the GMTKN55 data set. The Fock exchange term is calculated using vdW-DF-cx orbitals.

	$\Delta E^{\text{ref}}$	$\Delta E^{\text{cx}}$	$\Delta E^{\text{tlh}}$	$\Delta E^{\text{cx0}}$	$\Delta E^{\text{cx0p}}$	$a_{\text{sys}}$
Ammonia dimer	3.133	2.63	2.79	2.87	2.82	0.20
Water dimer	4.989	4.57	4.77	4.86	4.80	0.21
Formic acid dimer	18.753	18.65	19.38	19.64	19.42	0.21
Formamide dimer	16.062	14.93	15.72	15.91	15.71	0.21
Uracil dimer h-bonded	20.641	19.01	19.78	20.04	19.82	0.20
2-pyridoxine 2-aminopyridine complex	16.934	16.88	17.13	17.32	17.22	0.18
Adenine-thymine Watson-Crick complex	16.660	15.45	15.82	16.06	15.92	0.18
Average $a_{\text{sys}}$			Hydrogen Bonding			0.20
MD(kcal/Mol)		-0.72	-0.26	-0.07	-0.21	
MAD(kcal/Mol)		0.72	0.49	0.43	0.48	
MARD(%)		6.78	4.44	3.63	4.26	
Methane dimer	0.527	0.63	0.75	0.79	0.76	0.19
Ethene dimer	1.472	0.98	1.33	1.42	1.33	0.20
Benzene-methane complex	1.448	1.29	1.55	1.65	1.58	0.19
Benzene dimer parallel displaced	2.654	2.60	3.04	3.25	3.12	0.17
Pyrazine dimer	4.255	3.90	4.44	4.69	4.53	0.18
Uracil dimer stack	9.805	9.30	10.40	10.79	10.49	0.19
Indole-benzene complex stack	4.524	4.27	4.88	5.18	5.00	0.17
Adenine-thymine complex stack	11.730	10.84	12.15	12.69	12.31	0.18
Average $a_{\text{sys}}$			Dispersion Bonding			0.18
MD (kcal/Mol)		-0.33	0.27	0.51	0.34	
MAD (kcal/Mol)		0.35	0.30	0.52	0.37	
MARD (%)		11.60	11.98	16.53	13.54	
Ethene-ethyne complex	1.496	1.54	1.69	1.75	1.70	0.19
Benzene-water complex	3.275	2.94	3.30	3.41	3.32	0.20
Benzene-ammonia complex	2.312	2.06	2.36	2.46	2.38	0.19
Benzene-HCN complex	4.541	4.11	4.69	4.83	4.68	0.21
Benzene dimer T-shaped	2.717	2.55	2.93	3.09	2.98	0.18
Indole-benzene T-shape complex	5.627	5.24	5.80	6.01	5.86	0.18
Phenol dimer	7.097	6.29	6.92	7.14	6.97	0.19
Average $a_{\text{sys}}$			Mixed Bonding			0.19
MD (kcal/Mol)		-0.33	0.09	0.23	0.12	
MAD (kcal/Mol)		0.35	0.14	0.23	0.15	
MARD (%)		8.28	4.71	7.88	5.27	
Average $a_{\text{sys}}$			All S22 dimers			0.19
MD (kcal/Mol)		-0.45	0.04	0.24	0.09	
MAD (kcal/Mol)		0.47	0.31	0.40	0.34	
MARD (%)		9.01	7.27	9.68	7.95	

TABLE IV. Two-legged hybrid construction and comparison of performance for systems with pronounced intra-molecular noncovalent binding (IDISP), for covalent binding in aluminum complexes (A12X6), and for the Diels-Alder set of reaction energies (DARC). The geometries and reference energies for the IDISP (6 systems), A12X6 (6 systems), and DARC (14 systems) data sets are taken from Ref. 38. The values in square brackets are calculated with optimized geometries using the corresponding functionals—in the case of IDISP: including/excluding the C<sub>22</sub>H<sub>46</sub> unfolding case (the only case where there is any discernible relaxation effect, see Table S.VI–S.VIII of the [supplementary material](#)).

Reaction	$\Delta E^{\text{PBE0}}$	$\Delta E^{\text{cx}}$	$\Delta E^{\text{tlh}}$	$\Delta E^{\text{cx0}}$	$\Delta E^{\text{cx0p}}$
IDISP	$a = 0.25$	$a = 0$	$\langle a_{\text{sys}} \rangle = 0.18$	$a = 0.25$	$a' = 0.20$
MD (kcal/mol)	1.42	2.02[2.73/2.67]	1.01	0.78[1.30/0.75]	1.03[1.56/1.11]
MAD (kcal/mol)	9.77	2.36[2.73/2.67]	1.66	1.90[2.40/2.07]	1.75[2.32/2.03]
MARD (%)	241.98	31.52[50.64/29.97]	22.44	28.79[53.38/22.88]	24.00[51.11/22.59]
A12X6	$a = 0.25$	$a = 0$	$\langle a_{\text{sys}} \rangle = 0.20$	$a = 0.25$	$a' = 0.20$
MD (kcal/mol)	-3.29[-3.32]	-2.67[-2.67]	-1.70	-1.65[-1.67]	-1.86[-1.88]
MAD (kcal/mol)	3.29[3.32]	2.67[2.67]	1.70	1.65[1.67]	1.86[1.88]
MARD (%)	10.05[10.16]	6.81[6.81]	4.51	4.21[4.26]	4.75[4.81]
DARC	$a = 0.25$	$a = 0$	$\langle a_{\text{sys}} \rangle = 0.21$	$a = 0.25$	$a' = 0.20$
MD (kcal/mol)	1.06[1.08]	-0.84[-0.86]	-4.00	-4.74[-4.72]	-3.94[-3.94]
MAD (kcal/mol)	3.28[3.28]	1.70[1.70]	4.00	4.74[4.72]	3.94[3.94]
MARD (%)	12.80[12.82]	5.60[5.52]	12.49	15.39[15.35]	12.30[12.33]

$a_{\text{sys}}$  values around the average value 0.20, as detailed in the [supplementary material](#).

The description for IDISP is good already at the level of vdW-DF-cx (as further discussed below) and improves with the hybrid formulations. The two-legged hybrid constructions (“vdW-DF-tlh”) are better than the original vdW-DF-cx0 version and approach that of PBE0-D3, Ref. 38. The same trend is found also for the A12X6 set. The deviations for vdW-DF-cx and hybrids are larger but so is the average absolute energy, and the MARD values are smaller than those in the case of IDISP. Again the hybrid vdW-DF formulations, including vdW-DF-tlh, improve the description.

Previous studies have indicated that meta-GGA descriptions (with dispersion corrections as in SCAN-D3) perform better than at least traditional semilocal hybrids for the DARC set.<sup>38,95</sup> Here the regular vdW-DF-cx functional<sup>23</sup> performs very well. Use of the hybrid vdW-DF formulations worsens this performance, although the two-legged construction (“vdW-DF-tlh”) still performs at the level of PBE0 (Table IV).

We trust the vdW-DF-tlh analysis, summarized in Table IV, for all of the IDISP, A12X6, and DARC sets. Our trust builds on the observation that vdW-DF-cx, the original vdW-DF-cx0 version,<sup>6</sup> and a new zero-parameter (“0p”) specification, denoted as vdW-DF-cx0p and defined below, are all highly accurate in their characterization of structure. This is true for all of the A12X6 and DARC systems and all but one of the IDISP systems.

Tables S.VII and S.VIII of the [supplementary material](#) report results obtained at reference geometries as well as (inside square brackets) at fully relaxed geometries. There are no discernible structural relaxations in either of cx, cx0 (or cx0p) and consequently no relevant energy differences in the binding and reaction energies that we have obtained for A12X6 and DARC.

Figure 3 compares the structure result of a fully relaxed vdW-DF-cx calculation against that of the quantum-chemistry reference data<sup>38</sup> for the folded morphology of C<sub>22</sub>H<sub>46</sub>; There

are similar structure differences for vdW-DF-cx0 and vdW-DF-cx0p calculations. Such results are relevant for the last of the IDISP benchmark tests, namely, concerning C<sub>22</sub>H<sub>46</sub> unfolding. Table S.VI of the [supplementary material](#) documents that there is no observable relaxation effect in any of the first 5 benchmark cases of the IDISP benchmark set (as in all of the A12X6 and DARC cases).

The total relaxation effect on the results for the C<sub>22</sub>H<sub>46</sub> unfolding energy is found to be just 2-3 kcal/mol for the hybrid vdW-DF versions, Table S.VI of the [supplementary material](#). However, the relaxation does cause a change of sign for all of the vdW-DF-cx, vdW-DF-cx0, and vdW-DF-cx0p results (relative to the quantum-chemistry reference data<sup>38</sup>) for this particular case. The relaxation effects translate into a finite impact on the IDISP MARD value, Table IV. At the same time, the MARD increase with relaxations is still originating from just one structure, Fig. 3.

## B. Definition of a parameter-free hybrid: vdW-DF-cx0p

The vdW-DF-tlh analysis of the vdW-DF-cx0 design<sup>6</sup> motivates us to define a new version,

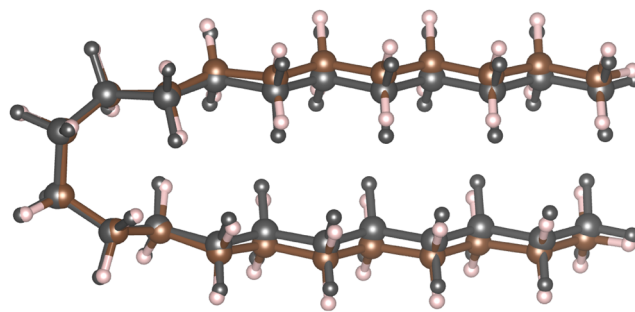


FIG. 3. Schematics of the folded C<sub>22</sub>H<sub>46</sub> system as described at the GMTKN55 reference geometries<sup>38</sup> (black) and at the geometry relaxed in vdW-DF-cx calculations (brown and white). This structure defines the last of the IDISP benchmarks and it is the only case of all of the IDISP, A12X6, and DARC systems where there are any discernible relaxations in vdW-DF-cx, vdW-DF-cx0, and vdW-DF-cx0p calculations (relative to the quantum-chemistry reference data on structure<sup>38</sup>).

$$E_{xc}^{cx0p} = a' E_x^{Fo} + (1 - a') E_x^{cx} + E_c^{cx}, \quad (21)$$

to enable self-consistent calculations for general molecular (covalent and noncovalent) interactions. The choice of the  $a' = 0.2$  value represents an optimal average value for general molecular interactions. A motivation for introducing this vdW-DF-cx0p version, Eq. (21), is that it can be seen as strictly free of adjustable parameters. It is parameter free in the sense that the mixing value  $a'$  is asserted from a formal analysis (i.e., our vdW-DF-tlh constructions) that reflects the expected ACF behavior of vdW-DF-cx.<sup>30</sup>

At the same time, it should be made clear that the two-legged construction vdW-DF-tlh clearly identifies some scatter in the set of suggested  $a_{sys}$  mixing values (even if concentrated around  $\langle a_{sys} \rangle = 0.2$ ). On the one hand, the scatter in  $a_{sys}$  could just be a consequence of vdW-DF-tlh not being self consistent. On the other hand, the scatter does suggest that the simple, unscreened hybrid vdW-DF-cx0 design, and the vdW-DF-cx0p version in particular, cannot be expected to be accurate for all types of molecular problems, let alone bulk-systems cases.

To provide an insight into the relevance of either of these possibilities, we are led to next explore the performance of the vdW-DF-cx0p version for molecular and some extended systems. A simple comparison of the vdW-DF-cx0p usefulness with that of vdW-DF-cx,<sup>23</sup> of vdW-DF-tlh (above), of the original vdW-DF-cx0 version,<sup>6</sup> and with that of other hybrids or vdW inclusive functionals can provide some guide lines for how to best continue the development of truly nonlocal-correlation hybrids like the vdW-DF-cx0 design. Also, it may be that while there is some scatter in the vdW-DF-tlh assessment of plausible  $a_{sys}$  values, there may not be a large impact of changing the Fock-exchange mixing in the vdW-DF-cx0 design. That is, the vdW-DF-cx0p version might provide a good all-round description of covalent and noncovalent interaction properties in any case.

### C. Robustness of the vdW-DF-cx0p: Molecular tests

We first note that Tables II–IV also include a raw summary of the vdW-DF-cx0p performance comparison for fixed geometries. Additional details for individual systems in the full G2-1, G2RC, G21IP, IDISP, A12X6, DARC, and S22

benchmark sets are given in the Tables S.VI–S.XII of the [supplementary material](#). We find that vdW-DF-cx0p performs on par with vdW-DF-tlh for both covalent and non-covalent binding properties, even if slightly worse in the case of atomization and dispersion energies. Moreover, vdW-DF-cx0p works on par with or improves the vdW-DF-cx0 performance for covalent binding properties. The vdW-DF-cx0p functional also improves the description of dispersion and mixed binding cases of S22, although slightly worsening the description of cases with a pronounced hydrogen bond.

Table V shows a comparison of the vdW-DF-cx and vdW-DF-cx0p performances for the S22 data set against so-called dispersion-corrected GGA descriptions: PBE-XDM,<sup>88,89</sup> PBE-D3,<sup>97</sup> and PBE-TS.<sup>98</sup> These are descriptions in which a pair-potential formulation of the vdW attraction is added to PBE. The numbers outside square parentheses reflect results obtained at reference geometries and we find that performance of vdW-DF-cx and vdW-DF-cx0p functionals, as measured in the MAD values, are comparable to those of the dispersion-corrected versions. This is true in spite of the fact that the group of dispersion-corrected functionals (PBE-XDM, PBE-D3, and PBE-TS) employ a damping function which is fitted to training sets that themselves include (or consist of) the S22 data set. The damping in the PBE-XDM and PBE-D3 versions is detailed, for example, in Ref. 38 and is broader than S22, comprising about 60 systems. For assessment of the S22 performance of vdW- or dispersion-corrected functionals, there are documented effects of focusing the training of the damping function on just the S22 set.<sup>89</sup> Our vdW-DF-cx and vdW-DF-cx0p functionals avoid such parameter issues completely, being set by formal many-body physics inputs<sup>21,24</sup> (including the ACF-based argument for picking the  $a' = 0.2$  mixing).

Table VI compares the MAD values that we here obtain for vdW-DF-cx0p (“cx0p”) against those obtained in PBE-D3, revPBE-D3, SCAN-D3, and PBE0-D3 in the GMTKN55 report<sup>38</sup> and against the results that we obtain in vdW-DF-cx and in the original vdW-DF-cx0 version.<sup>6</sup> Reference 38 highlights (rev)PBE-D3 and SCAN-D3 as good, all round choices on the lower rungs of functional approximations and PBE0-D3 represents a natural hybrid reference (being a

TABLE V. Performance of vdW-DF-cx and vdW-DF-cx0p for S22 data set compared with dispersion corrected DFT methods: PBE-XDM,<sup>88,89</sup> PBE-D3,<sup>97</sup> and PBE-TS.<sup>98</sup> The geometries are taken from Ref. 92 and the reference energies are taken from Ref. 93. The values in brackets are from fully relaxed calculations. In the lower part is the statistics of the binding distance for fully relaxed dimers. The PBE-XDM results are obtained using QUANTUM ESPRESSO with PAW pseudopotentials.<sup>87</sup>

	$\Delta E^{cx}$	$\Delta E^{cx0p}$	$\Delta E^{PBE-XDM}$	$\Delta E^{PBE-D3}$	$\Delta E^{PBE-TS}$
MD (kcal/mol)	−0.45[−0.60]	0.09[−0.31]	−0.41[−0.36]	−0.09[−0.20]	0.20[0.02]
MAD (kcal/mol)	0.47[0.68]	0.34[0.60]	0.59[0.54]	0.54[0.57]	0.34[0.49]
MARD (%)	9.01[9.43]	7.95[9.90]	9.75[8.40]	11.56[11.05]	10.01[12.83]
	$d^{cx} - d^{ref}$	$d^{cx0p} - d^{ref}$	$d^{PBE-XDM} - d^{ref}$	$d^{PBE-D3} - d^{ref}$	$d^{PBE-TS} - d^{ref}$
MD (Å)	0.058	0.034	0.064	0.061	0.018
MAD (Å)	0.068	0.044	0.075	0.073	0.040
MARD (%)	2.38	1.57	2.65	2.57	1.50

TABLE VI. Comparison of performance of vdW-DF-cx (“cx”), vdW-DF-cx0 (“cx0”), and vdW-DF-cx0p (“cx0p”) against that of dispersion-corrected functionals, PBE-D3, revPBE-D3, SCAN-D3, and PBE0-D3. The comparison is made for subsets of the GMTKN55 benchmark database.<sup>38</sup> The table reports mean absolute deviation (MAD) values in kcal/mol for calculations performed at reference geometries and against reference energies listed in Ref. 38. The statistics for the dispersion-corrected functionals are taken from Ref. 38 and are computed in an orbital-based approach, not the plane wave pseudopotential approach that we use here for the vdW-DF versions.

Reaction	$\Delta E^{\text{cx}}$	$\Delta E^{\text{cx0}}$	$\Delta E^{\text{cx0p}}$	$\Delta E^{\text{PBE-D3}}$	$\Delta E^{\text{revPBE-D3}}$	$\Delta E^{\text{SCAN-D3}}$	$\Delta E^{\text{PBE0-D3}}$
G2RC	6.16	4.01	4.24	6.92	6.16	6.39	6.75
G21IP	4.08	4.13	4.10	3.84	4.20	4.69	3.68
S22	0.47	0.40	0.34	0.48	0.43	0.47	0.48
IDISP	2.36	1.90	1.75	2.76	3.14	2.05	1.54
Al2X6	2.67	1.65	1.86	1.63	2.07	2.13	1.48
DARC	1.70	4.74	3.94	3.31	3.71	2.01	3.76

vdW-inclusive extension of a popular semilocal-correlation hybrid, PBE0). The comparison is made for the here-investigated GMTKN55 subsets and at listed reference geometries. Taken together, the set of benchmarks probes the ability of vdW-DF-cx and vdW-DF-cx0p to describe a range of molecular-interaction properties. As such, Table VI can be seen as a supplement to Ref. 76, which found that vdW-DF-cx performs significantly better for a broad comparison of molecule problems than both PBE-TS<sup>98</sup> and the so-called TS-MBD extension.<sup>100</sup>

We can only provide a qualitative discussion since, in contrast to our present cx0p/cx/cx0 plane wave calculations, the set of dispersion-corrected results is obtained in quantum-chemistry codes using quadruple- $\zeta$  atomic orbitals.<sup>38</sup> Nevertheless, we can observe that the vdW-DF-cx0p and vdW-DF-cx0 have the best performance for reaction energies. On average, the vdW-DF-cx and vdW-DF-cx0p perform at the same level as the listed set of dispersion-corrected functionals.

Figure 4 summarizes a comparison of PBE0, vdW-DF-cx, vdW-DF-cx0, and vdW-DF-cx0p performances for covalent, intra-molecular binding, using the aforementioned subsets of G2 and GMTKN55<sup>38,39</sup> but allowing for full structural approximations. The underlying data is given in the Tables S.VI–S.XI of the [supplementary material](#). The zero-parameter hybrid vdW-DF-cx0p performs better overall than PBE0 and vdW-DF-cx0 for these G2 and GMTKN55 subsets but the improvements are just moderate.

Next we contrast the performances for G2-1, G2RC, and G21IP in fully relaxed hybrid studies, Fig. 4, with those obtained using reference geometries, Table II. We find that both vdW-DF-cx0 and vdW-DF-cx0p characterizations for relaxed geometries are clearly better (essentially unchanged) for G2-1 (for G2RC and G21IP). This is somewhat in contrast to the behavior for vdW-DF-cx itself. For PBE0, there are only limited effects of including relaxations for G2-1, G2RC, and G21IP.

As already discussed in Subsection V A and as detailed in Table IV, we find that vdW-DF-cx, vdW-DF-cx0, and vdW-DF-cx0p all perform excellently for structure characterizations in the IDISP, Al2X6, and DARC sets. This is encouraging for the vdW-DF-cx and hybrid vdW-DF-cx formulations since these cases are included in the GMTKN55<sup>38</sup>

to test the ability of functionals to describe the effect of intra-molecular charge relocation on weaker binding energies.<sup>38</sup>

Figure 3 shows the structure of the folded C<sub>22</sub>H<sub>46</sub> system. As mentioned above, this is the one case where the vdW-DF-cx and hybrid vdW-DF-cx structure results differ from the reference data among the IDISP/Al2X6/DARC benchmarks (Tables S.VI–S.VIII of the [supplementary material](#)). We note that the IDISP benchmark subset is itself small,<sup>38</sup> and it is relevant to assert the extent that this single difference affects our vdW-DF-cx/vdW-DF-cx0p benchmarking for the IDISP set. Accordingly, we include in Table IV a summary of benchmarking with fully relaxed IDISP results while both including and excluding this special C<sub>22</sub>H<sub>46</sub> unfolding case; if the special case is omitted, we find again a good vdW-DF-cx and

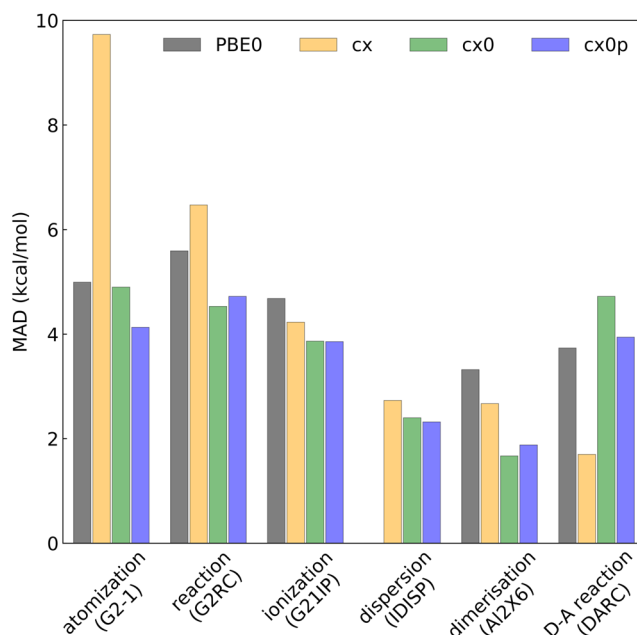


FIG. 4. Comparison of PBE0, vdW-DF-cx (cx), vdW-DF-cx0 (cx0), and vdW-DF-cx0p (cx0p) performances for binding properties of small molecules, for the G2-1 subsets of the G2 set<sup>39</sup> and for the G2RC, G21IP, IDISP, Al2X6, and DARC subsets of the GMTKN55 benchmark set.<sup>38</sup> We compare the mean-average deviations that reflect fully relaxed results, measured against the reference energy data.

vdW-DF-cx0p performance for IDISP, even when characterized in terms of the MARD values.

The comparison of vdW-DF-cx and vdW-DF-cx0 performances for the DARC deserves a separate discussion. The DARC set probes description of systems with multiple bonds and this is a class of systems where the vdW-DF-cx already performs very well, Fig. 4. However, comparing the vdW-DF-cx MD and MAD values for the DARC set in Table IV, it is also clear that vdW-DF-cx provides a systematic underestimation of the DARC energies. Since, furthermore, the use of vdW-DF-cx0p systematically decreases these reaction energies, we end up with a worse performance for vdW-DF-cx0p. Our finding that the DARC set challenges vdW-DF-cx0p is consistent with previous findings that semilocal-correlation hybrids perform worse than, for example, meta-GGA based descriptions for the DARC set.<sup>95</sup>

In the case of non-covalent inter-molecular bonding, there is a potential for more pronounced geometry relaxations (not reflected in Table III) to play a role. For example, in the S22 set of molecular dimers, the binding energies are small and the geometries can be significantly adjusted by forces. Computing binding energies at a fixed geometry need not provide a relevant description of the binding energy minima as described with a given (hybrid) functional. Thus ignoring relaxation might prevent us from learning if the functional in question is strongly over-binding.

The top panels of Fig. 5 illustrate the procedure that we provide for a revised comparison of the performance for S22, going beyond the Table II comparison. In this, we follow the approach that we have also previously used, for example, in the recent paper launching the vdW-DF-cx0 hybrid vdW-DF design.<sup>6</sup> We begin with reference dimer geometries, which in

the S22 benchmark case are extracted from a series of increasingly more accurate quantum chemistry calculations, ending with an interpolation among coupled cluster (CC) studies for geometries located around the expected energy minimum. We next adjust the inter-molecular separations inwards and outwards in steps of 0.025 Å and obtain a binding curve for vdW-DF-cx, for vdW-DF-cx0, and for vdW-DF-cx0p. Finally, we extract both the molecular-dimer binding separation  $d$  and binding energy estimates  $\Delta E$  relative to the S22 reference data,  $d_{CC}$  and  $\Delta E_{CC}$ .

The top panels also reveal the importance of including structural relaxations. While a comparison at the  $d_{CC}$  geometry works well (for regular and hybrid vdW-DF-cx) in the case of hydrogen bonded systems (like the water dimer) and in the case of mixed bonding (like the water-benzene complex), it leads to an underestimation of the binding energy in systems (like the benzene-benzene complex) with a pure dispersion bonding. This is one good reason to use vdW-DF-cx0p instead of vdW-DF-tlh.

The bottom panel of Fig. 5 shows the full comparison of performances for vdW-DF-cx, vdW-DF-cx0, and vdW-DF-cx0p; the underlying data is listed in Table S.XII of the [supplementary material](#). The upper (lower) half of this panel reports the variation in  $d - d_{CC}$  (in  $\Delta E - \Delta E_{CC}$ ). We have (as in Table III) separated the survey into cases reflecting hydrogen bonding, dispersion bonding, and mixed bonding. As also observed in Ref. 6, we find that hybrid vdW-DF-cx (vdW-DF-cx0 and vdW-DF-cx0p) is accurate for hydrogen and mixed bonding cases but less accurate for the cases with a pure dispersion bonding.

Table V also includes a characterization of the vdW-DF-cx0p performance for S22 using the approximate

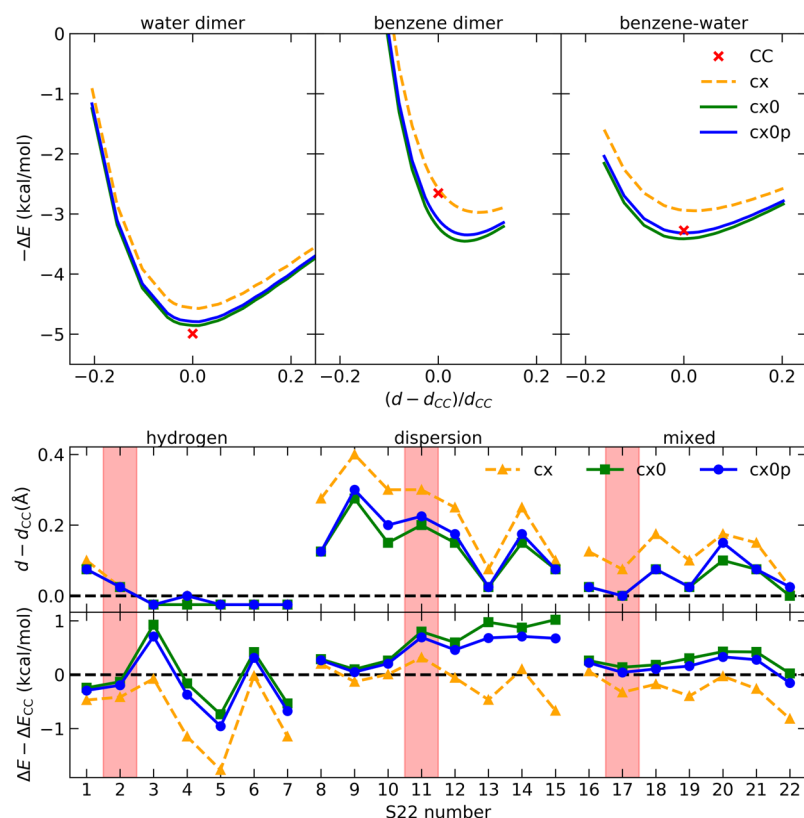


FIG. 5. Comparison of performance of vdW-DF-cx, of vdW-DF-cx0, and of vdW-DF-cx0p for (inter-molecular) noncovalent binding in the S22 data set.<sup>92,99</sup> The top panel illustrates how, in this performance comparison, we partly include the effects of geometry relaxations, computing (for each functional) binding-energy curves as we decrease or increase the inter-molecular separation relative to the S22 reference (marked by a cross). The bottom panels compare the functional-specific results for the binding separation  $d$  and the binding energy  $\Delta E$ , respectively. The variation is plotted relative to the S22 reference values,  $d_{CC}$  and  $\Delta E_{CC}$ .

determination of relaxation effects, Fig. 5. That is, the table includes a characterization of binding energies (inside square brackets in the top half) and of optimal binding separations (with average deviations listed in the bottom Table part); further detail is included in Table S.XII of the [supplementary material](#). When focused on relaxed calculations (for S22), we find that vdW-DF-cx0p improves the vdW-DF-cx description, especially in terms of binding separations. The performances of the strictly parameter-free vdW-DF-cx and vdW-DF-cx0p functionals are also comparable to those of the dispersion-corrected versions (PBE-XDM, etc).

Taken overall, our analysis demonstrates that the vdW-DF-cx0 design is robust toward small changes in the Fock-exchange mixing. While the use of vdW-DF-cx0p does improve the description over the vdW-DF-cx0, the improvement is not dramatic. At the same time, we find that the vdW-DF-cx0p version does have a good average choice for the exchange mixing  $a' = 0.2$ , one that works for both covalent and noncovalent molecular binding.

This choice  $a' = 0.2$  is, of course, already in wide use for traditional molecular investigations, for example, used in the construction of so-called optically tuned range-separated hybrids (OTRSH).<sup>101</sup> However, we have documented here that  $a' = 0.2$  is also motivated and applicable in the new vdW-DF-cx0 design<sup>6</sup> which can therefore provide concurrent descriptions of general types of molecular interactions.

#### D. Robustness of vdW-DF-cx0p: Extended systems

The vdW-DF-cx0 design also aims to be useful for systems comprising both molecules and bulk. We therefore include a comparison of vdW-DF-cx0 (at  $a = 0.25$ ) and

vdW-DF-cx0p (at  $a' = 0.2$ ) performances for a few extended systems.

Table VII contrasts the PBE, PBE0, vdW-DF-cx, vdW-DF-cx0, and vdW-DF-cx0p descriptions of the cubic-cell lattice constant  $b$ , the cohesive energy  $E_{\text{coh}}$ , and bulk modulus  $B$  for a set of traditional semiconductors (and related insulators): C, Si, SiC, and GaAs. The listed experimental values for  $b$  and  $E_{\text{coh}}$  are corrected for vibrational zero-point energy and thermal effects, as available in Ref. 40. Hybrids are expected to behave reasonable for the description of bulk semiconductors and PBE0 generally improves the description of PBE. Similarly, while the vdW-DF-cx characterization is already at the level of PBE or better, the hybrid vdW-DF-cx formulations provide bulk-semiconductor descriptions that are accurate for the structure, cohesion, and elastic properties. This suggests that vdW-DF-cx0p may also serve us for a parameter-free description of molecules on a semiconducting substrate.

Simple hybrids (like PBE0 or the vdW-DF-cx0 design) should not generally be used for the description of conducting systems because they rely on the inclusion of the Fock exchange and thus lack an inherent account of screening. Nevertheless, we include in Table VII a comparison of structure, cohesion-energy, and elastic-response characterizations for a few second-row transition metals. Again, zero-point energy and thermal corrections on the experimental numbers are included from Ref. 40, where available.

One of us has previously documented that the regular nonlocal-correlation functional vdW-DF-cx is itself highly accurate for characterizations of the thermo-physical properties of non-magnetic transition-metal elements,<sup>70</sup>

TABLE VII. Comparison of vdW-DF-cx (abbreviated “cx”), vdW-DF-cx0 (“cx0”), and vdW-DF-cx0p (“cx0p”) performances for bulk semiconductors and a few second-row transition metals: cubic-cell lattice constant  $b$  (in Å), cohesive energy  $E_{\text{coh}}$  (in eV), and bulk modulus  $B$  (in GPa). Reference energies are experimental values corrected (except for  $B$ ) by an estimate for zero-point energy corrections, as listed in Ref. 40.

		PBE	PBE0	cx	cx0	cx0p	Reference
C	$b$	3.572	3.553	3.561	3.550	3.552	3.543
	$E_{\text{coh}}$	7.671	7.505	7.841	7.572	7.618	7.583
	$B$	430	463	440	467	463	443
Si	$b$	5.464	5.441	5.437	5.430	5.431	5.416
	$E_{\text{coh}}$	4.504	4.558	4.743	4.723	4.766	4.681
	$B$	89	99	93	101	100	99
SiC	$b$	4.374	3.352	4.358	4.346	4.348	4.342
	$E_{\text{coh}}$	6.368	6.353	6.590	6.489	6.542	6.488
	$B$	210	229	217	232	229	225
GaAs	$b$	5.745	5.645	5.680	5.608	5.622	5.638
	$E_{\text{coh}}$	3.130	3.191	3.408	3.411	3.407	3.393
	$B$	60	76	67	80	77	76
Rh	$b$	3.837	3.791	3.789	3.764	3.768	3.793
	$E_{\text{coh}}$	5.939	4.111	6.407	4.496	4.814	5.784
	$B$	247	281	283	304	300	269
Pd	$b$	3.945	3.917	3.884	3.879	3.878	3.875
	$E_{\text{coh}}$	3.790	2.862	4.337	3.296	3.499	3.918
	$B$	170	170	202	190	196	195
Ag	$b$	4.165	4.166	4.075	4.106	4.099	4.056
	$E_{\text{coh}}$	2.524	2.322	2.897	2.635	2.683	2.972
	$B$	84	80	108	94	97	109

Table VII (with results obtained here using a different code) confirms this observation.

Table VII furthermore shows that the vdW-DF-cx0 and vdW-DF-cx0p versions remain usable for some properties, specifically for structure. Not surprisingly, the cohesive energies worsen, although the vdW-DF-cx0p version performs better in this regard than both PBE0 and vdW-DF-cx0. However, the fact that the structure characterizations remain accurate for these transition metals is promising. This suggests that vdW-DF-cx0p remains at least relevant for descriptions of molecular adsorption subjected to full relaxation, as is often necessary.<sup>53,67</sup>

Finally, we note that a full discussion of the extended systems, and especially of the metals, requires attention to the questions of screening exchange contributions. The vdW-DF-cx0p is a completely unscreened hybrid and so we are presently over-estimating the effects of long-range exchange. Improvements relative to the vdW-DF-cx0 design<sup>6</sup> are motivated and could take the form of adapting the HSE<sup>102,103</sup> or OTRSH<sup>101</sup> logic to the vdW-DF framework.

## VI. SUMMARY AND CONCLUSION

Adapting the motivation for PBE-based hybrids,<sup>11,12</sup> we have constructed system-specific two-legged hybrids vdW-DF-tlh based on the vdW-DF-cx coupling-constant variation.<sup>30</sup> The vdW-DF-tlh constructions are related to the idea of a perturbation-theory approach to hybrid density functionals;<sup>10,11,13</sup> It combines calculations of the functional coupling-constant variation and MP2 results to establish the Fock mixing fraction  $a \approx 1/m$  ( $m$  integer) directly.<sup>10</sup> The two-legged hybrid constructions<sup>12</sup> provide a qualitative discussion of this strictly parameter-free perturbation-based hybrid approach. We emphasize that the vdW-DF-tlh design is not suggested for pursuing broad calculations; it is for analysis only.

Our overall discussion is based on using vdW-DF-tlh for molecular problems: subsets of the G2-1 atomization energy,<sup>39</sup> the G2RC set of reaction-energies,<sup>95</sup> the G2IIP set of ionization-potentials,<sup>95</sup> the S22 set of inter-molecular binding benchmarks,<sup>92,99</sup> the IDISP set of intra-molecular noncovalent interactions,<sup>38</sup> the A12X6 set of aluminum dimerization energies,<sup>38,95</sup> and the DARC set of Diels-Alder reaction energies. The IDISP, A12X6, and DARC energies all test effects of electron affinities and delocalization errors. While lacking self consistency, we find that the vdW-DF-tlh is accurate. This builds confidence in our qualitative results: (a) the plausible all-round value for a hybrid vdW-DF-cx0 design would be  $a = 0.2$ , close to but different from the  $a = 0.25$  value that was used in Ref. 6, but also, (b) there is only a partial rationale for just using single, fixed Fock-exchange mixing fraction in Eq. (1) since there is a scatter in the values that we extract from trying to use vdW-DF-tlh.

As an interesting aside, we note that the vdW-DF-tlh analysis can be used to check if, in some specific problem, a given choice of the Fock mixing is very off for the hybrid use, for example, very different from the typical recommendations for hybrids,<sup>82</sup>  $a = 0.25$  or  $a' = 0.2$ . This analysis can be made using our code `PPACF` for tracking the coupling-constant variation of the vdW-DF-cx functional (and other

semilocal- or nonlocal-correlation density functionals), as evaluated for system-specific, self-consistent electron-density solutions.<sup>30</sup>

Our analysis leads us to explore a specific version, termed vdW-DF-cx0p, of the vdW-DF-cx0 design.<sup>6</sup> This is done, because unlike vdW-DF-tlh, the vdW-DF-cx0p (with fixed mixing  $a' = 0.2$ ) can be carried to self-consistency. We find that vdW-DF-cx0p, compared to the original vdW-DF-cx0 form (having  $a = 0.25$ ), generally improves the description of molecular systems, as expected by the vdW-DF-tlh analysis.

We suggest using the vdW-DF-cx0p version (of the vdW-DF-cx0 design<sup>6</sup>) for both covalent and noncovalent molecular systems. We make this suggestion because vdW-DF-cx0p can be seen as restricting all parameter inputs to formal many-body perturbation theory: Even the assessment of an optimal average mixing value  $a' = 0.2$  comes from analysis of the vdW-DF-tlh constructions (which, in turn is based on the analysis of ACF behavior for the underlying strictly parameter-free vdW-DF-cx). We also observe that the vdW-DF-tlh analysis does indicate a finite scatter in relevant  $a_{\text{sys}}$  values for general hybrid characterizations of molecular interactions. We see this scatter as, in part, expected from the long tradition in using traditional semilocal-correlation hybrids.<sup>5,11-13,82</sup>

The vdW-DF-cx0p usefulness originates, in practice, from our present demonstration that a single, fixed value  $a' = 0.2$  can be used for a concurrent description of both covalent and noncovalent interactions in molecules. In addition, we find that it is useful in some extended-system cases. The vdW-DF-cx0 design<sup>6</sup> is robust and there are only moderate effects of changing the Fock-exchange mixing.

It is interesting that our present vdW-DF-tlh-based identification of an optimal average mixing value,  $a' = 0.2$ , for the vdW-DF-cx0 design<sup>6</sup> is identical to the value Becke originally extracted for standard semilocal-correlation hybrids.<sup>1</sup> The  $a' = 0.2$  value is in broad usage for molecular problems, for example, in the definition the OTRSH<sup>101</sup> that can reliably track electronic excitations. Becke's identification of  $a'$  is based on a fit, comparing results from a range of potential semilocal-correlation hybrids to mostly covalent interaction properties of molecules (and some atom problems). By contrast, the present specification is based on a formal ACF-based analysis<sup>10-12,27,30</sup> for the underlying regular vdW-DF-cx functional.

We view the fact that there are two independent but coinciding specifications of  $a' = 0.2$  as an indication of a soundness in the logic of nonlocal-correlation hybrid functionals. The vdW-DF-cx can formally be seen as a systematic extension of semilocal GGA functionals,<sup>24,32</sup> with a seamless integration. The vdW-DF-cx construction secures a highly reliable traditional-material description in cases with a dense electron distribution.<sup>33,62,66,70</sup> Such cases include covalent bonding in molecules. It is therefore possible to view the present work both as a formal rediscovery of the Becke  $a' = 0.2$  mixing value and as a demonstration that it extends to noncovalent molecular binding as well. The demonstration is important because vdW-DF-cx0 has a different design logic than the traditional semilocal-correlation hybrids.

## SUPPLEMENTARY MATERIAL

See [supplementary material](#) for 12 tables, denoted as S.I–S.XII, individually introduced and referenced in the text above. The supplementary-material tables detail the two-legged hybrid constructions as well as the vdW-DF-cx, vdW-DF-cx0, vdW-DF-cx0p, and PBE0 performances for individual molecular systems or reactions in the G2-1, G2RC, G21IP, S22, IDISP, A12X6, and DARC benchmark sets. As such, they provide the basis for our assessment of an optimum average mixing ratio  $\langle a_{\text{sys}} \rangle$  and for the performance comparisons that we summarize in Tables I–VII (and in Figs. 4 and 5).

## ACKNOWLEDGMENTS

We thank Kristian Berland, Jung-Hoon Lee, Tonatiuh Rangel, Zhenfei Liu, and Jeffrey B. Neaton for discussions. This work is supported by the Swedish Research Council (VR) through Grant Nos. 2014-4310 and 2014-5289 and by the Chalmers Area-of-Advance-Materials theory activity. Computational resources were provided by the Swedish National Infrastructure for Computing (SNIC), under Contract No. 2016-10-12, and by the Chalmers Centre for Computing, Science and Engineering (C3SE), under Contract Nos. C3SE 605/16-4 and C3SE2018-1-10.

- 1 A. D. Becke, *J. Chem. Phys.* **98**, 5648 (1993).
- 2 C. Adamo and V. Barone, *J. Chem. Phys.* **110**, 6158 (1999).
- 3 K. Kim and K. D. Jordan, *J. Phys. Chem.* **98**, 10089 (1994).
- 4 P. J. Stephens, F. J. Devlin, C. F. Chabalowski, and M. J. Frisch, *J. Phys. Chem.* **98**, 11623 (1994).
- 5 A. D. Becke, *J. Chem. Phys.* **140**, 18A301 (2014).
- 6 K. Berland, Y. Jiao, J.-H. Lee, T. Rangel, J. B. Neaton, and P. Hyldgaard, *J. Chem. Phys.* **146**, 234106 (2017).
- 7 D. C. Langreth and J. P. Perdew, *Solid State Commun.* **17**, 1425 (1975).
- 8 O. Gunnarsson and B. I. Lundqvist, *Phys. Rev. B* **13**, 4274 (1976).
- 9 D. C. Langreth and J. P. Perdew, *Phys. Rev. B* **15**, 2884 (1977).
- 10 A. Görling and M. Levy, *Phys. Rev. B* **47**, 13105 (1993).
- 11 J. P. Perdew, M. Ernzerhof, and K. Burke, *J. Chem. Phys.* **105**, 9982 (1996).
- 12 K. Burke, M. Ernzerhof, and J. P. Perdew, *Chem. Phys. Lett.* **265**, 115 (1997).
- 13 M. Ernzerhof, J. P. Perdew, and K. Burke, *Int. J. Quantum Chem.* **64**, 285 (1997).
- 14 D. C. Langreth and J. P. Perdew, *Phys. Rev. B* **21**, 5469 (1980).
- 15 D. C. Langreth and M. J. Mehl, *Phys. Rev. Lett.* **47**, 446 (1981).
- 16 J. P. Perdew and Y. Wang, *Phys. Rev. B* **33**, 8800 (1986).
- 17 J. P. Perdew and Y. Wang, *Phys. Rev. B* **46**, 12947 (1992).
- 18 J. P. Perdew, K. Burke, and M. Ernzerhof, *Phys. Rev. Lett.* **77**, 3865 (1996).
- 19 J. P. Perdew, A. Ruzsinszky, G. I. Csonka, O. A. Vydrov, G. E. Scuseria, L. A. Constantin, X. Zhou, and K. Burke, *Phys. Rev. Lett.* **100**, 136406 (2008).
- 20 M. Dion, H. Rydberg, E. Schröder, D. C. Langreth, and B. I. Lundqvist, *Phys. Rev. Lett.* **92**, 246401 (2004).
- 21 T. Thonhauser, V. R. Cooper, S. Li, A. Puzder, P. Hyldgaard, and D. C. Langreth, *Phys. Rev. B* **76**, 125112 (2007).
- 22 O. A. Vydrov and T. Van Voorhis, *J. Chem. Phys.* **133**, 244103 (2010).
- 23 K. Berland and P. Hyldgaard, *Phys. Rev. B* **89**, 035412 (2014).
- 24 P. Hyldgaard, K. Berland, and E. Schröder, *Phys. Rev. B* **90**, 075148 (2014).
- 25 T. Thonhauser, S. Zuluaga, C. A. Arter, K. Berland, E. Schröder, and P. Hyldgaard, *Phys. Rev. Lett.* **115**, 136402 (2015).
- 26 H. Peng, Z.-H. Yang, J. Sun, and J. P. Perdew, *Phys. Rev. X* **6**, 041005 (2016).
- 27 M. Levy and J. P. Perdew, *Phys. Rev. A* **32**, 2010 (1985).
- 28 M. Levy, *Phys. Rev. A* **43**, 4637 (1991).
- 29 M. Levy, in *Density Functional Theory*, edited by E. K. U. Gross and R. M. Dreizler (Plenum Press, 1995), pp. 11–31.
- 30 Y. Jiao, E. Schröder, and P. Hyldgaard, *Phys. Rev. B* **97**, 085115 (2018).
- 31 J. P. Perdew, K. Burke, and Y. Wang, *Phys. Rev. B* **54**, 16533 (1996).
- 32 K. Berland, V. R. Cooper, K. Lee, E. Schröder, T. Thonhauser, P. Hyldgaard, and B. I. Lundqvist, *Rep. Prog. Phys.* **78**, 066501 (2015).
- 33 K. Berland, C. A. Arter, V. R. Cooper, K. Lee, B. I. Lundqvist, E. Schröder, T. Thonhauser, and P. Hyldgaard, *J. Chem. Phys.* **140**, 18A539 (2014).
- 34 Y. Jiao, F. Zhang, M. Grätzel, and S. Meng, *Adv. Funct. Mater.* **23**, 424 (2013).
- 35 X. Wang, K. Esfarjani, and M. Zebarjadi, *J. Phys. Chem. C* **121**, 15529 (2017).
- 36 K. Berland, E. Londero, E. Schröder, and P. Hyldgaard, *Phys. Rev. B* **88**, 045431 (2013).
- 37 K. Burke and L. O. Wagner, *Int. J. Quantum Chem.* **113**, 96 (2013).
- 38 L. Goerigk, A. Hansen, C. Bauer, S. Ehrlich, A. Najibi, and S. Grimme, *Phys. Chem. Chem. Phys.* **19**, 32184 (2017).
- 39 L. A. Curtiss, K. Raghavachari, P. C. Redfern, and J. A. Pople, *J. Chem. Phys.* **106**, 1063 (1997).
- 40 G. I. Csonka, J. P. Perdew, A. Ruzsinszky, P. H. T. Philipsen, S. Lebègue, J. Paier, O. A. Vydrov, and J. G. Ángyán, *Phys. Rev. B* **79**, 155107 (2009).
- 41 H. Rydberg, M. Dion, N. Jacobson, E. Schröder, P. Hyldgaard, S. I. Simak, D. C. Langreth, and B. I. Lundqvist, *Phys. Rev. Lett.* **91**, 126402 (2003).
- 42 K. Lee, E. D. Murray, L. Kong, B. I. Lundqvist, and D. C. Langreth, *Phys. Rev. B* **82**, 081101 (2010).
- 43 G. D. Mahan, *J. Chem. Phys.* **43**, 1569 (1965).
- 44 A. C. Maggs and N. W. Ashcroft, *Phys. Rev. Lett.* **59**, 113 (1987).
- 45 K. Rapcewicz and N. W. Ashcroft, *Phys. Rev. B* **44**, 4032 (1991).
- 46 Y. Andersson, D. C. Langreth, and B. I. Lundqvist, *Phys. Rev. Lett.* **76**, 102 (1996).
- 47 M. Dion, H. Rydberg, E. Schröder, D. C. Langreth, and B. I. Lundqvist, *Phys. Rev. Lett.* **95**, 109902(E) (2005).
- 48 V. R. Cooper, *Phys. Rev. B* **81**, 161104 (2010).
- 49 J. Klimeš, D. R. Bowler, and A. Michaelides, *J. Phys.: Condens. Matter* **22**, 022201 (2010).
- 50 J. Klimeš, D. R. Bowler, and A. Michaelides, *Phys. Rev. B* **83**, 195131 (2011).
- 51 I. Hamada, *Phys. Rev. B* **89**, 121103 (2014).
- 52 G. Román-Pérez and J. M. Soler, *Phys. Rev. Lett.* **103**, 096102 (2009).
- 53 A. Hjorth Larsen, M. Kuisma, J. Löfgren, Y. Pouillon, P. Erhart, and P. Hyldgaard, *Modell. Simul. Mater. Sci. Eng.* **25**, 065004 (2017).
- 54 F. Tran, J. Stelzl, D. Koller, T. Ruh, and P. Blaha, *Phys. Rev. B* **96**, 054103 (2017).
- 55 D. C. Langreth, B. I. Lundqvist, S. D. Chakarova-Käck, V. R. Cooper, M. Dion, P. Hyldgaard, A. Kelkkanen, J. Kleis, L. Kong, S. Li, P. G. Moses, E. Murray, A. Puzder, H. Rydberg, E. Schröder, and T. Thonhauser, *J. Phys.: Condens. Matter* **21**, 084203 (2009).
- 56 J. Klimeš and A. Michaelides, *J. Chem. Phys.* **137**, 120901 (2012).
- 57 O. A. Vydrov and T. Van Voorhis, *Phys. Rev. Lett.* **103**, 063004 (2009).
- 58 R. Sabatini, T. Gorni, and S. de Gironcoli, *Phys. Rev. B* **87**, 041108(R) (2013).
- 59 K. Berland, “Connected by voids: Interactions and screening in sparse matter,” Ph.D. thesis, Department of Microtechnology and Nanoscience – MC2, Chalmers University of Technology, Göteborg, Sweden, 2012.
- 60 K. Berland and P. Hyldgaard, *Phys. Rev. B* **87**, 205421 (2013).
- 61 T. Björkman, *J. Chem. Phys.* **141**, 074708 (2014).
- 62 P. Erhart, P. Hyldgaard, and D. Lindroth, *Chem. Mater.* **27**, 5511 (2015).
- 63 R. C. Clay, M. Holzmann, D. M. Ceperley, and M. A. Morales, *Phys. Rev. B* **93**, 035121 (2016).
- 64 A. Ambrosetti and P. L. Silvestrelli, *Phys. Rev. B* **94**, 045124 (2016).
- 65 M. Hellström, I. Beinik, P. Broqvist, J. V. Lauritsen, and K. Hermansson, *Phys. Rev. B* **94**, 245433 (2016).
- 66 D. O. Lindroth and P. Erhart, *Phys. Rev. B* **94**, 115205 (2016).
- 67 J. Löfgren, H. Grönbeck, L. Moth-Poulsen, and P. Erhart, *J. Phys. Chem. C* **120**, 12059 (2016).
- 68 T. Rangel, K. Berland, S. Sharifzadeh, F. Brown-Altwater, K. Lee, P. Hyldgaard, L. Kronik, and J. B. Neaton, *Phys. Rev. B* **93**, 115206 (2016).
- 69 F. Brown-Altwater, T. Rangel, and J. B. Neaton, *Phys. Rev. B* **93**, 195206 (2016).
- 70 L. Gharraee, P. Erhart, and P. Hyldgaard, *Phys. Rev. B* **95**, 085147 (2017).
- 71 G. G. Kebede, D. Spångberg, P. D. Mitev, P. Broqvist, and K. Hermansson, *J. Chem. Phys.* **146**, 064703 (2017).
- 72 P. A. T. Olsson, E. Schröder, P. Hyldgaard, M. Kroon, E. Andreasson, and E. Bergvall, *Polymer* **121**, 234 (2017).
- 73 B. Borca, T. Michnowicz, R. Petuya, M. Pristl, V. Schendel, I. Pentegov, U. Kraft, H. Klauk, P. Wahl, R. Gutzler, A. Arnau, U. Schlickum, and K. Kern, *ACS Nano* **11**, 4703 (2017).

- <sup>74</sup>I. Cabria, M. J. Lopez, and J. A. Alonso, *J. Chem. Phys.* **146**, 214104 (2017).
- <sup>75</sup>I. Loncaric, J. Popovic, V. Despoja, S. Burazer, I. Grgicevic, D. Popovic, and Z. Skoko, *Cryst. Growth Des.* **17**, 4445 (2017).
- <sup>76</sup>J. Claudot, W. J. Kim, A. Dixit, H. Kim, T. Gould, D. Rocca, and S. Lebegue, *J. Chem. Phys.* **148**, 064112 (2018).
- <sup>77</sup>M. Fritz, M. Fernandez-Serra, and J. M. Soler, *J. Chem. Phys.* **144**, 224101 (2016).
- <sup>78</sup>B. Borca, V. Schendel, R. Petuya, I. Pentegov, T. Michnowicz, U. Kraft, H. Klauk, A. Arnau, P. Wahl, U. Schlickum, and K. Kern, *ACS Nano* **9**, 12506 (2015).
- <sup>79</sup>M. Wang, J.-Q. Zhong, J. Kestell, I. Waluyo, D. J. Stacchiola, A. J. Boscoboinik, and D. Lu, *Top. Catal.* **60**, 481 (2017).
- <sup>80</sup>P. Nozières and D. Pines, *Phys. Rev.* **111**, 442 (1958).
- <sup>81</sup>L. Hedin and B. I. Lundqvist, *J. Phys. C* **4**, 2064 (1971).
- <sup>82</sup>K. Burke, *J. Chem. Phys.* **136**, 150901 (2012).
- <sup>83</sup>P. Giannozzi, S. Baroni, N. Bonini, M. Calandra, R. Car, C. Cavazzoni, D. Ceresoli, G. L. Chiarotti, M. Cococcioni, I. Dabo, A. D. Corso, S. de Gironcoli, S. Fabris, G. Fratesi, R. Gebauer, U. Gerstmann, C. Gougoussis, A. Kokalj, M. Lazzeri, L. Martin-Samos, N. Marzari, F. Mauri, R. Mazzarello, S. Paolini, A. Pasquarello, L. Paulatto, C. Sbraccia, S. Scandolo, G. Sclauzero, A. P. Seitsonen, A. Smogunov, P. Umari, and R. M. Wentzcovitch, *J. Phys.: Condens. Matter* **21**, 395502 (2009).
- <sup>84</sup>P. Giannozzi, O. Andreussi, T. Brumme, O. Bunau, M. Buongiorno Nardelli, M. Calandra, R. Car, C. Cavazzoni, D. Ceresoli, M. Cococcioni, N. Collonna, I. Carnimeo, A. Dal Corso, S. de Gironcoli, P. Delugas, R. A. DiStasio, Jr., A. Ferretti, A. Floris, G. Fratesi, G. Fugallo, R. Gebauer, U. Gerstmann, F. Giustino, T. Gorni, J. Jia, M. Kawamura, H.-Y. Ko, A. Kokalj, E. Küçükbenli, M. Lazzeri, M. Marseli, N. Marzari, F. Mauri, H.-V. Nguyen, A. Otero-de-la Roza, L. Paulatto, S. Poncé, D. Rocca, R. Sabatini, B. Santra, M. Schlipf, A. Seitsonen, A. Smogunov, I. Timrov, T. Thonhauser, P. Umari, N. Vast, X. Wu, and S. Baroni, *J. Phys.: Condens. Matter* **29**, 465901 (2017).
- <sup>85</sup>N. Troullier and J. L. Martins, *Phys. Rev. B* **43**, 1993 (1991).
- <sup>86</sup>X. Gonze, M. Rignanese, M. Verstraete, J. M. Beuken, Y. Pouillon, R. Caracas, F. Jollet, M. Torrent, G. Zerah, M. Mikami, P. Ghosez, M. Veithen, J. Y. Raty, V. Olevanov, F. Bruneval, L. Reining, R. Godby, G. Onida, D. R. Hamann, and D. C. Allen, *Z. Kristall* **220**, 558 (2005).
- <sup>87</sup>G. Kresse and D. Joubert, *Phys. Rev. B* **59**, 1758 (1999).
- <sup>88</sup>A. D. Becke and E. R. Johnson, *J. Chem. Phys.* **127**, 154108 (2007).
- <sup>89</sup>A. O. de-la Roza and E. R. Johnson, *J. Chem. Phys.* **136**, 174109 (2012).
- <sup>90</sup>D. R. Hamann, *Phys. Rev. B* **88**, 085117 (2013).
- <sup>91</sup>L. Lin, *J. Chem. Theory Comput.* **12**, 2242 (2016).
- <sup>92</sup>P. Jurecka, J. Sponer, J. Cerny, and P. Hobza, *Phys. Chem. Chem. Phys.* **8**, 1985 (2006).
- <sup>93</sup>M. S. Marshall, L. A. Burns, and C. D. Sherrill, *J. Chem. Phys.* **135**, 194102 (2011).
- <sup>94</sup>Fock-exchange mixing values  $a = 1/m$  for  $m > 6$  is not considered relevant.<sup>12</sup>
- <sup>95</sup>L. Goerigk and S. Grimme, *J. Chem. Theory Comput.* **6**, 107 (2010).
- <sup>96</sup>J. Sun, A. Ruzsinszky, and J. P. Perdew, *Phys. Rev. Lett.* **115**, 036402 (2015).
- <sup>97</sup>S. Grimme, J. Antony, S. Ehrlich, and H. Krieg, *J. Chem. Phys.* **132**, 154104 (2010).
- <sup>98</sup>A. Tkatchenko and M. Scheffler, *Phys. Rev. Lett.* **102**, 073005 (2009).
- <sup>99</sup>T. Takatani, E. G. Hohenstein, M. Malagoli, M. S. Marshall, and C. D. Sherrill, *J. Chem. Phys.* **132**, 144104 (2010).
- <sup>100</sup>A. Tkatchenko, R. A. DiStasio, R. Car, and M. Scheffler, *Phys. Rev. Lett.* **108**, 236402 (2012).
- <sup>101</sup>S. Refaely-Abramson, M. Jain, S. Sharifzadeh, J. B. Neaton, and L. Kronik, *Phys. Rev. B* **92**, 081204 (2015).
- <sup>102</sup>J. Heyd, G. E. Scuseria, and M. Ernzerhof, *J. Chem. Phys.* **118**, 8207 (2003).
- <sup>103</sup>J. Heyd, G. E. Scuseria, and M. Ernzerhof, *J. Chem. Phys.* **124**, 219906 (2006).